École Nationale Polytechnique

Département d'Automatique

المدرسة الوطنية المتعددة التقنيات
Ecole Nationale Polytechnique

Laboratoire de Commande des Processus

End of studies project thesis

Submitted in partial fulfillment of the requirements
for the State Engineer Degree in Automation Engineering

Fault tolerant fuzzy control of the safety distance of an electric vehicle in traffic

Realized by:
Mr. EL GAMAH Ahmed Wassim

Supervised by:
Mr. ACHOUR Hakim
Mr. BOUKHETALA Djamel

Publicly presented and defended on the 14th of July, 2022.

Jury members:

President	Mr. Omar STIHI	MAA	ENP
Promoters	Mr. Hakim ACHOUR	MAA	ENP
	Mr. Djamel BOUKHETALA	Pr	ENP
Examiner	Mr. Djamel BOUDANA	Pr	ENP

ENP 2022

École Nationale Polytechnique

Département d'Automatique

End of studies project thesis

Submitted in partial fulfillment of the requirements
for the State Engineer Degree in Automation Engineering

Fault tolerant fuzzy control of the safety distance of an electric vehicle in traffic

Realized by:
Mr. El Gamah Ahmed Wassim

Supervised by:
Mr. Achour Hakim
Mr. Boukhetala Djamel

Publicly presented and defended on the 14ᵗʰ of July, 2022.

Jury members:

President	Mr. Omar Stihi	MAA	ENP
Promoters	Mr. Hakim Achour	MAA	ENP
	Mr. Djamel Boukhetala	Pr	ENP
Examiner	Mr. Djamel Boudana	Pr	ENP

ENP 2022

École Nationale Polytechnique

Département d'Automatique

Ecole Nationale Polytechnique

المدرسة الوطنية المتعددة التقنيات

Laboratoire de Commande des Processus

Mémoire de projet de fin d'études

pour l'obtention du diplôme d'Ingénieur d'État en Automatique

Commande floue tolérante aux défauts de la distance de sécurité d'un véhicule électrique en circulation

Réalisé par :
M. El Gamah Ahmed Wassim

Supervisé par:
Mr. Achour Hakim
Mr. Boukhetala Djamel

Présenté et soutenue publiquement le 14 Juillet 2022.

Membres du jury :

Président	M. Omar Stihi	MAA	ENP
Promoteurs	M. Hakim Achour	MAA	ENP
	M. Djamel Boukhetala	Pr	ENP
Examinateur	M. Djamel Boudana	Pr	ENP

ENP 2022

ملخص

الموضوع الرئيسي لمشروع نهاية الدراسة هذا هو التحكم المتسامح مع الأخطاء للأنظمة غير الخطية الموصوفة بنماذج ضبابية. نقدم أولاً بعض المعلومات العامة عن السيارات الكهربائية ، ثم نعطي نموذجها الديناميكي. نقدم بعد ذلك بعض النتائج لتحليل النماذج الضبابية وكيفية دراسة استقرارها. نقدم أيضًا النتائج الرئيسية المتعلقة بشروط استقرار هته النماذج بواسطة منظم ارجاع الحالات مع وجود ملاحظ و مع غيابه. تتم كتابة شروط الاستقرار لنماذج الضبابية في متباينات المصفوفة الخطية . استخدمنا طرق إعادة بناء الحالة وتقدير الأخطاء مع مراقب ، ثم تم تطوير منظم نشط يتحمل الأخطاء من أجل التحكم في المسافة بين السيارات.

كلمات مفتاحية : سيارة كهربائية, متباينة مصفوفية خطية, نماذج ضبابية, تحكم متسامح مع الأخطاء.

Résumé

Le sujet principal de ce projet de fin d'étude est la commande tolérante aux défuts pour des systèmes non linéaires décrits par des modèles flous de Takagi-Sugeno. Nous présentons d'abord quelques généralités sur les véhicules électriques, puis nous donnons leur modèle dynamique. Nous présentons ensuite quelques résultats pour l'analyse des modèles flous T-S et comment étudier leur stabilité. Nous présentons également les principaux résultats concernant le problème de la stabilisation des modèles T-S par un régulateur à retour d'état flou avec la présence et l'absence d'observateur d'état. Les conditions de stabilité des modèles flous T-S sont écrites en inégalités matricielles linéaires (IML). Nous avons utilisé des méthodes de reconstruction de l'état et d'estimation des défauts avec un observateur PI, puis un régulateur actif tolérant aux défauts a été développé afin de contrôler la distance inter-véhiculaire.

Mots clés : Véhicule électrique, inégalité matricielle linéaire (IML), modèles flous Takagi-Sugeno, commande tolérante aux défauts.

Abstract

The main subject of this project thesis is the fault tolerant control of nonlinear systems described by Takagi-Sugeno fuzzy models. We present firstly some generalities about electrical vehicles and then we give their dynamic model. We present after that some results for the analysis of T-S fuzzy models and how to study their stability. We also present the main results concerning the stabilization problem of T–S models by a fuzzy state feedback controller with the presence and the absence of state observer. The stability conditions of the T–S fuzzy models are written in linear matrix inequalities (LMIs). Then, a structure with integral part to assure path tracking.We used reconstruction methods of state and faults estimation with PI observer, then an active fault tolerant control was developed in order to control the vehicle spacing.

Keywords : Electrical vehicle, Linear matrix inequality (LMI), Takagi-Sugeno fuzzy models, Fault tolerant control.

Dedication

Acknowledgments

First of all, I would like to thank all the people who contributed to the success of my studies and who helped me in the writing of this work.

Words cannot express my gratitude to my supervisors, Mr. Hakim ACHOUR and Mr. Djamel BOUKHETALA for their invaluable patience, feedback and guidance during the journey of this thesis.

I would also like to extend my thanks in advance to Mr. STIHI and Mr. BOUDANA, for evaluating my project.

I am also grateful to all my teachers who impacted and inspired me throughout my academic curriculum. Thanks should also go to my classmates, especially my friend Amine BOUDJOGHRA for his editing help, feedback session and moral support.

Lastly, I would be remiss in not mentioning my family, especially my parents. Their belief in me has kept my spirits and motivation high during this process. I would also like to thank my cat for all the entertainment and emotional support.

Contents

List of Figures

List of Abbreviations

EV	*Electric vehicule*
TS	*Takagi Sugeno*
LMI	*Linear Matrix Inequality*
LTI	*Linear time invariant*
PDC	*Parallel distribution compenstion*
FTC	*Fault tolerant control*
AFTC	*Actif fault tolerant control*
PFTC	*Passif fault tolerant control*
FDI	*Fault detectiong and isolation*
DOS	*Dedicated Observer Scheme*
GOS	*Generalized Observer Scheme*
PI	*Proportional Integral*
PMI	*Proportional Multi Integral*

General Introduction

The number of classic vehicles circulating in the world has continued to increase since their invention. Indeed, the number of accidents continues to rise, claiming many victims every year. In addition, the use of vehicles with internal combustion engines is having more and more harmful effects on the environment. Therefore, the development of electrically powered vehicles has become one of the major concerns of researchers around the world. The research carried out in this direction, based on on power electronics and energy storage materials have helped the transition to the electric vehicle. energy storage materials have favored the transition to the electric vehicle respectful of the the environment.

In fact, at the beginning of its launch, the electric vehicle was designed to reduce environmental risks, so road safety was the next challenge for car manufacturers and research organizations. In this regard, many automatic safety systems have been proposed to avoid traffic accidents or reduce their severity and thus save hundreds of thousands of human lives. Thanks to the technological progress and the integration of modern automation, the control systems in the electric vehicle have known significant advances especially in the last decades in order to ensure a good road handling, a high stability and sometimes a low cost of ownership. high stability and sometimes automatic braking of the vehicle.

In automation, like almost all physical systems, the electric vehicle is classified as a nonlinear dynamic system, which is governed by nonlinear differential equations describing the temporal evolution of the system's constituent variables under the effect of independent variables called inputs or control variables, with the objective of obtaining the desired output signals. The interactions between the components of the system and the existing non-linearities are the reason of the complexity of such systems. In these systems, the notion of transfer functions is no longer valid in the models describing them. Therefore, linear control theory is no longer useful. The use of nonlinear control approaches is necessary. Nevertheless, the number of available nonlinear approaches remains limited. Among the methods currently used is the notion of fuzzy systems of the Takagi-Sugeno type. These systems allow to approximate a large class of nonlinear systems. In the context of this thesis, we will use these systems for the control of systems for the control of the inter-vehicle distance in traffic.

This thesis is composed of four chapters and is organized in the following way:

The first chapter is dedicated to the presentation of some generalities about the electric vehicle. We start by presenting the electric vehicle. We also mention its advantages and disadvantages, then we describe its architecture and its various constituent parts. Finally,

a longitudinal model of the vehicle used for the control application is explained.

The second chapter discusses the definition of the Takagi-Sugeno model and the different methods used for the construction of T-S multi-models from the dynamic equations. The linear sector method is explained in detail in order to exploit it for the synthesis of the controller of the system using the state feedback called the PDC method. After that, we present the control structure with integrator allowing a trajectory tracking. Stabilization conditions without and with state observer are also given. Finally, we present the LMI regions to make the desired pole placement ensuring the desired stability and performance in closed loop.

In the third chapter, some basic notions of nonlinear system diagnosis using the Takagi-Sugeno multi-model approach are presented. The methods of detection, localization and estimation of faults affecting a nonlinear system are described and based on PI observers. Then, the notion of fault tolerance and its different techniques are presented. The result of the fault estimation is used, afterwards, to design the FTC block, that enables to compensate the faults or to reconfigure the control law so that the performances are kept.

In the last chapter, we present results of the application of T-S fuzzy logic on the model used. We are interested in some aspects that show the performance of the implemented control such as the inter-vehicular distance, velocity and torque provided. The stabilization method discussed in chapter 2 and the fault tolerant control techniques presented in chapter 3 will also be applied and their results will be presented.

Finally, a general conclusion, followed by the bibliography and appendices end this manuscript.

Chapter 1

Generalities and presentation of the model of the electric vehicle

1.1 Introduction

Currently, almost all car manufacturers are committed to building their electric cars. Electric vehicles have become more and more important, as they do not produce any pollution and noise unlike conventional vehicles. Moreover, they are easy to model, which makes their control easier from the automatic point of view.

The number of vehicles on the road is continuously increasing from year to year. Therefore, the risk of traffic accidents has become very high. In order to reduce this risk, there are more and more electronic and automatic systems that are integrated in the vehicles to avoid or at least minimize these accidents.
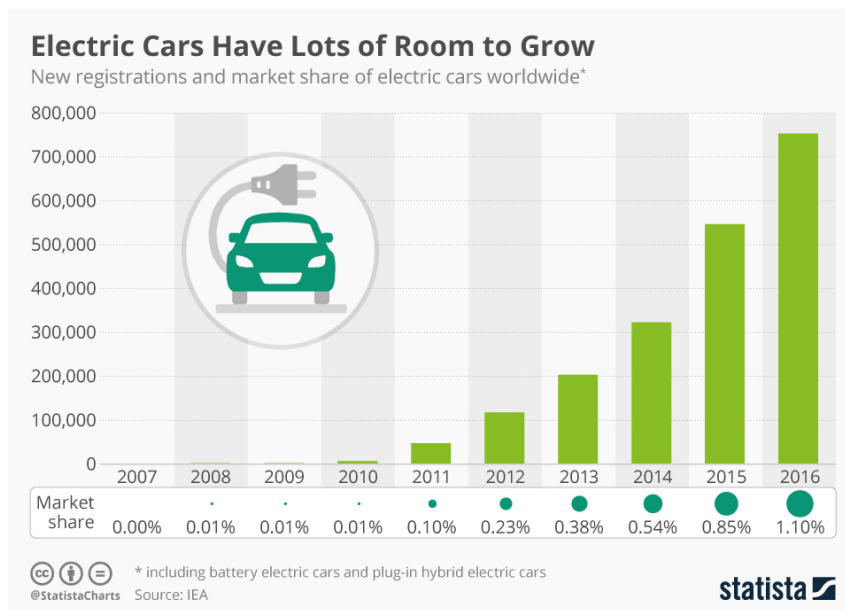
Figure 1.1: Number of electric vehicles in the world

In this chapter, we present generalities on electric vehicles starting with the definition of the electric car, its history and its architecture. Then, we present the longitudinal model used by our fuzzy control law to regulate the safety distance between vehicles.

1.2 Definition of electric vehicle

An electric vehicle is a vehicle that uses one or more electric motors for propulsion. It can be powered by a collector system, with electricity from extravehicular sources, or it can be powered autonomously by a battery (sometimes charged by solar panels, or by converting fuel to electricity using fuel cells or a generator).EVs include, but are not limited to, road and rail vehicles, surface and underwater vessels, electric aircraft and electric spacecraft.

Figure 1.2: electric vehicles around the world

1.3   History of electric vehicles

The history of electric cars can be broken up into five distinct periods: the early pioneers of electric mobility (1830-1880), the transition to motorized transport (1880-1914), the rise of the internal combustion engine (1914-1970), the return of electric vehicles (1970-2003), the electric revolution (2003-2020), and the tipping point (2021 and beyond).[1]
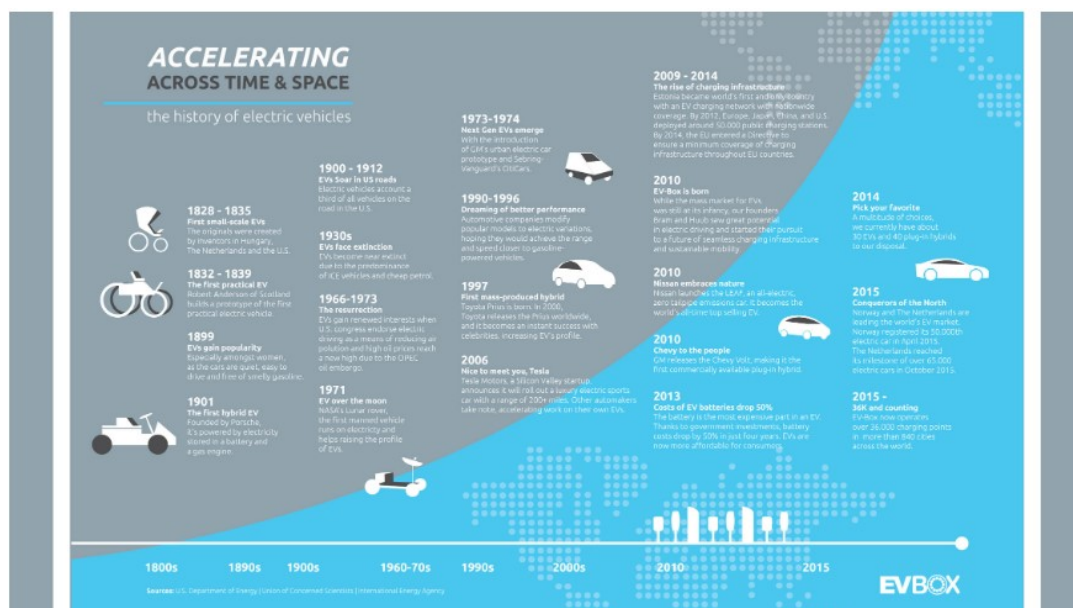
Figure 1.3: The history of electric vehicle

The early pioneers of electric mobility (1830-1880):

As early as the 1830s, inventors in Hungary, the Netherlands, the UK, and the US were focusing their efforts on combining these technological advances to create a powered motor vehicle. The first small-scale electric vehicle were developed by William Sturgeon in 1832.

The first electric vehicle was displayed at an industry conference in 1835 by a British

inventor by the name of Robert Anderson. Robert Anderson's vehicle used a disposable battery powered by crude oil to turn the wheels.

However, all were little more than prototypes of electrified carts—travelling at top speeds of 12 km/h with cumbersome steering, and little range. Then in the 1860s, a French physicist by the name of Gaston Plante invented the first rechargeable lead-acid battery— a huge breakthrough for electric mobility. Yet, it was until the late 1880s that these inventions batteries and electric motors were put together by electric mobility pioneer William Morrison to create the first "practical" EV.

Figure 1.4: The first electric car

The transition to motorized transport (1880-1914):

Around the turn of the 20th century, many people began swapping in their horses and carts for motorized vehicles. As a result, the automobile rapidly grew in popularity and the battle for the future of mobility commenced. The options were Steam, gasoline, or electric.

Steam vehicles had been growing in popularity since the 1870s and held a slim majority over the US market at the turn of the century, yet they had major setbacks which ultimately led to their downfall. Steam vehicles required startup times up to 45 minutes and continuously needed to be refilled with water, limiting their range. In the end, while steam was reliable for powering factories and trains, it proved not to be very practical for personal vehicles.

Around the same time as William Morrison was working on his electric-powered carriage, Gottlieb Daimler and Carl Benz simultaneously developed the world's first automobiles in 1886 in Germany. However, gasoline-powered cars required the driver to change gears and start the vehicle with a heavy hand crank. They were also far noisier than their steam or electric cousins and emitted pollutants from their exhausts.

In comparison to the two other vehicle types on the market, electric cars proved to be a competitive option. They did not emit any of the unpleasant pollutants, require changing gears, or have long startup times. This meant that they were easier to drive and they were much quieter too.

As a result, electric cars quickly became popular with urban residents where electricity was readily available and as more people gained access to electricity, the more popular they became. This popularity caught the eye of many pioneers of the day: Porsche de-

veloped the world's first hybrid car while Thomas Edison even partnered with friend and former employee Henry Ford to build an affordable EV.

Although, this momentum would all come to a slow end, with the creation of Ford's cost-efficient assembly line and the wider availability of gasoline.

The rise of the internal combustion engine (1914-1970):

EVs entered their darkest hour when the mass-produced internal combustion engine (ICE) vehicle was introduced. Along with Ford's Model T, gasoline-powered cars became widely available and affordable.

And after the discovery of oil in Texas, gasoline became cheap and readily available for many, while electricity only remained available in cities. Over the next 30 years, electric vehicles saw little advancement and by the mid-1930s, they had almost completely disappeared from the market.

Cheap, abundant gasoline and continued improvements to the internal combustion engine hampered demand for alternative fuel vehicles and solidified gasoline vehicles' dominance. As a result, the electric vehicle lay dormant for the better half of a century.

The return of electric vehicles (1970-2003):

Fast forward to the seventies, as oil prices and gasoline shortages reached a new high—peaking with the 1973 Arab Oil Embargo—interest in lowering the society's dependence on oil grew.

Automakers, feeling this social shift, started to explore options for alternative fuel vehicles, including electric cars. For instance, General Motors developed a prototype for an urban EV and even NASA helped raise the profile when their electric Lunar rover became the first manned vehicle on the moon. However, electric vehicles still suffered from several drawbacks compared to gasoline-powered cars including limited range and slow top speeds and consumers were not interested.

Yet, the lack of public interest didn't discourage scientists and engineers from trying. Over the next 20 years, automotive companies modified popular models to create electric variations, hoping they could improve the batteries and achieve a range and speed closer to that of gasoline-powered vehicles.

One of the most significant turning points was the introduction of the Toyota Prius. Released in Japan in 1997, the Prius became the world's first mass-produced hybrid electric vehicle. In 2000, the Prius was released worldwide, and it became an instant success with celebrities. Since then, rising gasoline prices and growing concern over carbon pollution have helped make the Prius the best-selling hybrid worldwide. However, the real turning point would come in 2003, when two entrepreneurs by the names of Martin Eberhard and Marc Tarpenning saw an opportunity.

The revolution (2003-2020):

After seeing the growth of lithium-ion battery capacity in their previous venture, Eberhard and Marc formed Tesla Motors in 2003. Fast forward to 2006, and the Silicon Valley startup had announced it would start producing a luxury electric sports car that could

go more than 320 km on a single charge.

Tesla's subsequent success spurred many big automakers to accelerate work on their own electric vehicles. Nissan raised the competition with its launch of the Nissan LEAF in 2010. This all-electric, zero-emission car would become the world's all-time top-selling EV.

At the same time, new battery technologies entered the market, helping to improve range and cutting EV battery costs. To demonstrate this, the price of lithium-ion batteries has declined by 97% since 1991. This, in turn, has helped lower the cost of electric vehicles overall, making them more affordable for consumers.

In the years since, almost every mass-market automotive manufacturer has hopped on the electric bandwagon and many have vowed to stop building the internal combustion engine altogether.

Figure 1.5: A modern electric car

1.4 Advantages and disadvantages of electric vehicles

Advantages

- The total absence of gas emissions, which makes the vehicle very ecological.

- The very low noise level of the vehicle.

Disadvantages

- A mass power limited by the batteries.

- a low autonomy.

Thus, the electric vehicle seems to be well adapted for small urban vehicles. Indeed, they are not too penalized by the limitation of power and range and the problem of gas and noise pollution is essential for them.[2]

1.5 Components of an electric vehicle

The main components of an EV can be divided into the electric battery,the electric motor, and a motor controller (Figure 1.6). The technical structure of an EV is simpler compared to internal combustion engine vehicle since no starting, exhaust or lubrication system, mostly no gearbox, and sometimes, not even a cooling system are needed.

The battery charges with electricity either when plugged in the electricity grid via a charging device or during braking through recuperation. The charger is a crucial component since its efficiency can vary today between 60% and 97%, wasting 3% to 40% of the grid energy as heat. The motor controller supplies the electric motor with variable power depending on the load situation. The electric motor converts the electric energy into mechanical energy and, when used within a drive-train, to torque. In series EV produced so far, central engines have been used; however, hub wheel electric engines are also possible and would be available for mass production. [3]

There are several types of electric motors, usually divided into alternating current (AC) and direct current (DC) types. There are both AC and DC electric engines built with and without permanent magnets, according to individual use.

There are several electric engines available, conventional mechanically commuted DC machines, the asynchronous machines, the load-controlled synchronous machines with electrical excitation, and the switched reluctance motors.
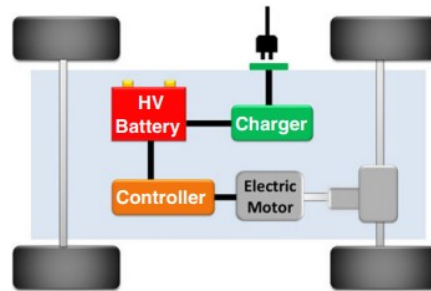
Figure 1.6: Important components of an electric car

1.6 Modelisation of an electric car

In the case where we are only interested in the control of the vehicle moving in a straight line, we have :
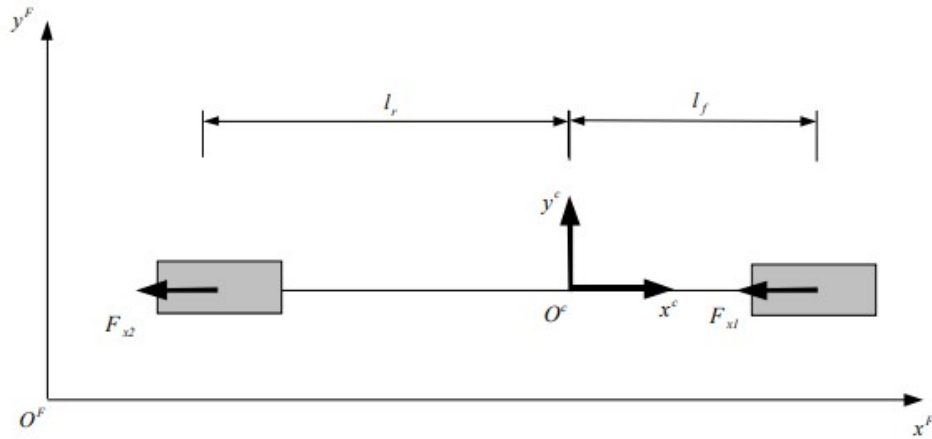
Figure 1.7: Representation of the vehicle to obtain a longitudinal model

1.6.1 Notations

The index 1 designates the front wheel of the vehicle and the index 2 the rear wheel. We show the main notations used in this section:

$\ddot{x}(t),\ \dot{x}(t)$:   Acceleration (m/s^2) and longitudinal velocity (m/s^2) of the vehicle.

$F_A(t)$:   Cumulative longitudinal forces of contact between the tires and the road (N)

F_{xres} :   Longitudinal aerodynamic force (N)

$F_x(t)$:   Longitudinal traction force of the tire contact with the road (N)

$F_z(t)$:   Reaction force of the tire to the vertical load (N)

$V_v(t)$:   The linear translation velocity of the wheel contact point with the road (m/s)

$\omega_r(t)$:   The the angular velocity of rotation of the wheel (rad/s)

R_r :   The rolling radius (m)

T_s :   Traction torque of the wheel (N.m)

T_e :   The torque supplied by the electric machine (N.m)

R_g :   The reduction ratio assumed of the gearbox and the differential

m :   Mass of the vehicle (Kg)

I_z :   Inertia along the vertical axis of the vehicle ($kg.m^2$)

l_f: Distance between the center of gravity of the vehicle and the axis of the front axle (m)

l_r: Distance between the center of gravity of the vehicle and the axis of the rear axle (m)

J_r :   Inertia of the wheel ($kg.m^2$)

J_e :   Inertia of the electric machine ($kg.m^2$)

a_x, b_x :   Longitudinal aerodynamic coefficients ($kg.m^2$) (kg)

S_x :   Longitudinal sliding of the wheel

μ_x :   Lateral adhesion coefficient

C :   Stiffness coefficient

1.6.2   Forces applied to wheels

The main forces acting on the wheel are the longitudinal traction force F_x which is opposite to the direction of travel of the vehicle, the lateral guidance force F_y which is opposite to the direction of travel of the wheel (it is zero in the case of longitudinal movement) and the reaction of the wheel to the vertical load F_z. To these forces, we can add the moments along the vertical axis M_z and lateral M_y.
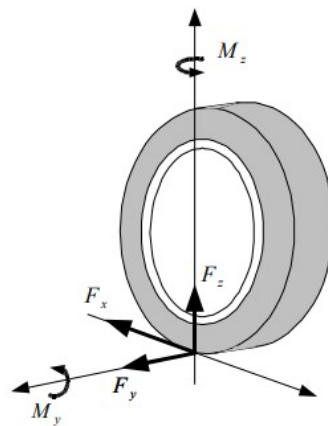
Figure 1.8: Forces and moments applied to the wheels

1.6.3   Longitudinal behavior of the wheel

The main phenomenon involved in the calculation of the longitudinal force is the longitudinal sliding.

1.6.3.1   Longitudinal sliding

The longitudinal sliding is due to the difference between the speed of translation of the center of the wheel and its wheel and its point of contact with the ground :
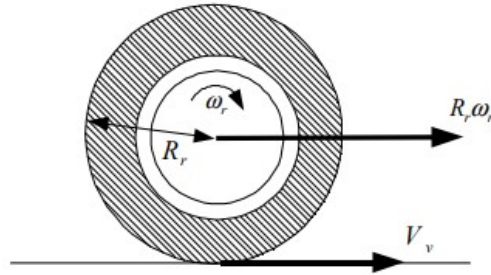
Figure 1.9: Difference between central and radial wheel speeds

Classically, the expression of longitudinal sliding is defined as a function of the ratio between V_v and $\omega_r.R_r$.

1.6.3.2 Purely longitudinal tensile force

The longitudinal force F_x is the product of the longitudinal adhesion coefficient μ_x with the normal force F_z :

$$F_x = -\mu_x.F_z \tag{1.1}$$

The characteristic of the longitudinal adhesion coefficient μ_x is a function of the sliding longitudinal S_x.

1.6.4 Hypothesis

1- The road is considered flat and uniform, also the acceleration of the vehicle is sufficiently low so that the suspension movements are assumed to be negligible. The load distribution on the wheels is therefore assumed to be constant.

2- The torque of traction or braking available on the shaft of the front wheels is entirely described by the dynamics of the electric machine. This means the gearbox reduction ratio is assumed to be constant:

$$T_s = \frac{1}{R_g}.T_e \tag{1.2}$$

3- Under the "normal" conditions considered, the longitudinal adhesion coefficients evolve in a linear way with their respective sliding:

$$\mu_x = \frac{C}{F_z}.S \tag{1.3}$$

4- It is assumed that the behavior of the wheels of the same axle is similar. The dynamics of the wheels of the same axle can be described by a virtual wheel located at the center of gravity of the axle:

$$R_{ri}.\dot{w}_{ri} = \ddot{x} \tag{1.4}$$

1.6.5 Simulation Model

By applying the fundamental equations of dynamics (see figure 1.6):

$$m\ddot{x} = F_A - F_{xres} \tag{1.5}$$

with F_A: the cumulative contact forces between the tires and the road in the longitudinal direction, and F_{xres}: force of resistance to longitudinal displacement (aerodynamic forces, friction).

$$\begin{cases} F_A = -F_{x1} - F_{x2} \\ F_{xres} = a\dot{x} + b\dot{x}^2 \end{cases} \tag{1.6}$$

The drive train consists of an electric machine, a gearbox, a differential and universal joints:

Figure 1.10: Traction chain

The equivalent inertia of the whole drive train can be brought back to the front wheel :

$$J_1 = J_{r1} + \frac{J_e}{R_g^2} \tag{1.7}$$

The rotational acceleration $\dot{\omega}_{ri}$ of the wheels is obtained from the equation of the moments applied to the center of the wheel:

$$\begin{cases} J_1\dot{\omega}_{r1} = F_{xc1}.R_{r1} + T_{s1} \\ J_2\dot{\omega}_{r2} = F_{xc2}.R_{r2} \end{cases} \tag{1.8}$$

Substituting the equations (1.2),(1.4),(1.6),(1.7) and (1.8) in (1.5) and if we put :

$I_1 = \frac{J_{R1}.R_g^2 + J_e}{R_{r1}^2.R_g^2}, R_{ap} = \frac{1}{R_{r1}.R_g}, I_2 = \frac{R_g^2(J_{r2}+m.R_{r2}^2)}{R_g^2 R_{r2}^2}$ and $\alpha = I_1 + I_2$ we find :

$$\alpha\ddot{x} = R_{ap}.T_e - a_x\dot{x} - b_x\dot{x}^2 \tag{1.9}$$

The electric machine is controlled in torque, we can write its dynamic equation of the following form:

$$\dot{T}_e(t) = \frac{1}{\tau_e}.(-T_e(t) + u_e(t)) \tag{1.10}$$

Where $u_e(t)$ is the torque set point and τ_e its time constant.

The considered system consists of two vehicles supposed to drive in a straight line. The first vehicle, designated as the lead vehicle, is autonomous. It is followed by an electric vehicle, designated as the follower vehicle, which is fully automated. The objective of the following vehicle is to maintain a desired safe distance from the leading vehicle (Figure

1.11). Since the two vehicles are independent in terms of mechanical linkage and the following vehicle must be able to detect the movements of the leading vehicle. of the leading vehicle.
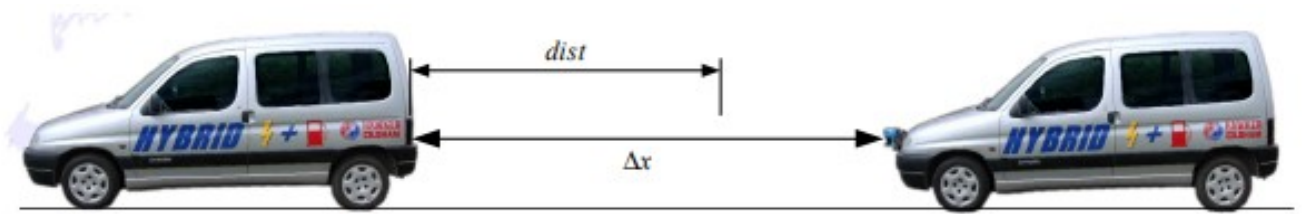
Figure 1.11: Vehicle configuration

Without inter-vehicular communications, an inter-distance set point that is dependent of the velocity is generally recommended and a set point with a constant safety factor, evolving quadratically with velocity, guarantees maximum safety. The inter-distance set point is therefore of the form :

$$dist(t) = d + e.\dot{x}(t) + f.\dot{x}(t)^2 \tag{1.11}$$

Where d is the minimum distance between the two vehicles, e can be interpreted as the reaction time and f allows to take into account the inertial effects and the braking capabilities of the vehicle.
We take: $e = 0.7s, f = 0.021s^2.m^{-1}, d = 2m$ [4]

The output considered is $y(t) = dist(t) - d$, and with the state vector $X(t) = \begin{bmatrix} \dot{x}(t) & T_e(t) \end{bmatrix}^T$, the longitudinal model of the EV , in the form of a state representation, is defined by :

$$\begin{cases} \dot{X}(t) = \begin{bmatrix} -\frac{a_x + b_x.\dot{x}(t)}{\alpha} & \frac{R_{ap}}{\alpha} \\ 0 & -\frac{1}{\tau_e} \end{bmatrix} .X(t) + \begin{bmatrix} 0 \\ \frac{1}{\tau_e} \end{bmatrix} u_e \\ y = \begin{bmatrix} e + f.\dot{x}(t) & 0 \end{bmatrix} X \end{cases} \tag{1.12}$$

The prototype hybrid vehicle used for the realization of the virtual coupling is a Citroën Berlingo equipped with a parallel hybrid powertrain. The latter is composed of a thermal engine with a maximum power of 55kW at 5800 rpm and a DC electric motor with separate excitation supplied in 240V and a maximum power of 43kW. 20 batteries of 12V-26Ah ensure the supply of the electric motor and the various control organs (jacks, computers, ...). The thermal engine can be uncoupled from the drive train thanks to a clutch. A reduction gearbox transmits the torque of the electric motor to the primary shaft of a two-speed velocity gearbox.

The parameters of the system are given by: [5]

a_x	14.55 kg. m /s
b_x	0.055 kg. m /s
R_{ap}	34.73
α	1860
τ	0.05 s
t_r	1 s
f	0.021

Figure 1.12: Table of parameters

The control objective is to ensure convergence of the inter-distance measurement Δx to the set point generated by equation (1.11). This is equivalent to bringing the output y of model (1.12) to $\Delta x - d$

1.7   Conclusion

In this chapter, we started by defining the electric vehicle, then we briefly discussed its history from its birth to the present day. Then, some advantages and disadvantages of this technology were mentioned. Then, we explained the functioning of the electric vehicle by specifying its architecture and the components of the traction chain. Finally, we presented the longitudinal model we presented the longitudinal model developed to control of the inter-vehicular distance.

Chapter 2

Stability of nonlinear systems described by Takagi Sugeno models

2.1 Introduction

In this chapter, we present the Takagi-Sugeno approach which is used to rewrite a non-linear system as a combination of linear systems weighted by nonlinear functions called activation functions. The interest of this method is to use the tools already known in the linear case to analyze the stability and synthesize a stabilizing controller for this kind of system. This is possible thanks to the convex sum property of the activation functions. These linear models weighted by normalized activation functions allow to represent without approximation the global non linear system.
In reality, we are not only interested in stabilizing the system but also in following a desired set point. In addition, the state of the system is rarely available, so an observer is synthesized to estimate the states of the system.

2.2 Concept of the TS fuzzy multi-model approach

The T-S approach is based on the decomposition of the dynamic behavior of the nonlinear system into a number r of operating domains, each domain is characterized by a linear sub-model. The figure 2.1 illustrates this principle in a two-dimensional case, with the set of operating points in the coordinate system $x(t) = (x_1(t), x_2(t))$has been decomposed into four operating domains denoted $C1, C2, C3$ and $C4$. The global operating domain is then defined by the union of the local domains $C = C_1 \cup C_2 \cup C_3 \cup C_4$.On each of the local domains, or subdomains, a local model can be constructed. The output of each sub model contributes more or less to the approximation of the global behavior of the nonlinear system. The contribution of each sub-model is defined by an activation function. These local models can then be be combined by means of an interpolation technique to obtain a global representation, or multi-model, valid on the global operating domain C.
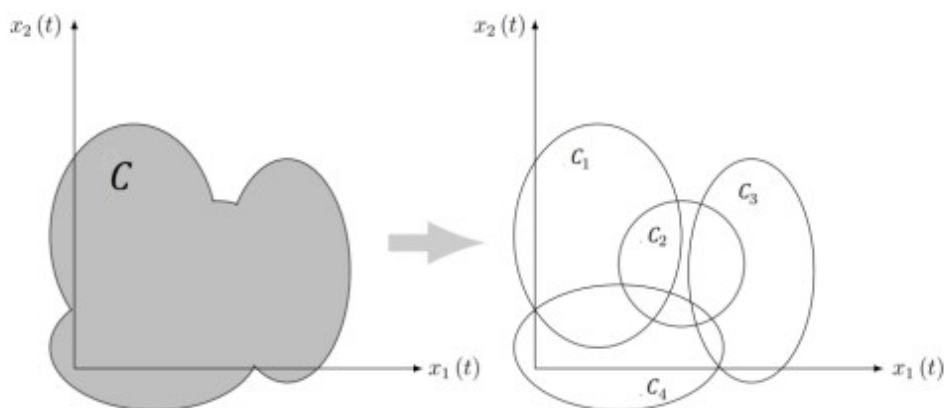
Figure 2.1: Principle of the Takagi-Sugeno approach

2.3 Takagi-Sugeno fuzzy model

2.3.1 Definition of TS model

Nonlinear systems can be written in the form of a TS model, this model is composed of a set of linear models weighted by nonlinear scalar functions (also called activation functions) which verify the property of the convex sum:

$$\begin{cases} \sum_{i=1}^{r} T_i(z(t)) = 1 \\ 0 \leq T_i(z(t)) \leq 1 \quad \forall t \end{cases} \tag{2.1}$$

With r the number of rules (or the number of models).
The TS model is:

$$\begin{cases} \dot{x}(t) = \sum_{i=1}^{r} T_i(z(t)).(A_i x(t) + B_i u(t)) \\ y(t) = \sum_{i=1}^{r} T_i(z(t)).(C_i x(t)) \end{cases} \tag{2.2}$$

With : $x(t) \in R^n$ is the state vector, $u(t) \in R^m$ is the input vector and $y(t) \in R^p$ is the output vector.
The r sub-models are defined by known matrices $A_i \in R^{n \times n}$, $B_i \in R^{n \times m}$ and $C_i \in R^{p \times n}$. The activation functions $T_i(z(t))$ are nonlinear functions depending on the parameter $z(t)$ that can be measurable (e.g., the input u(t) or the output y(t) of the system) or non-measurable (the state x(t) of the system).
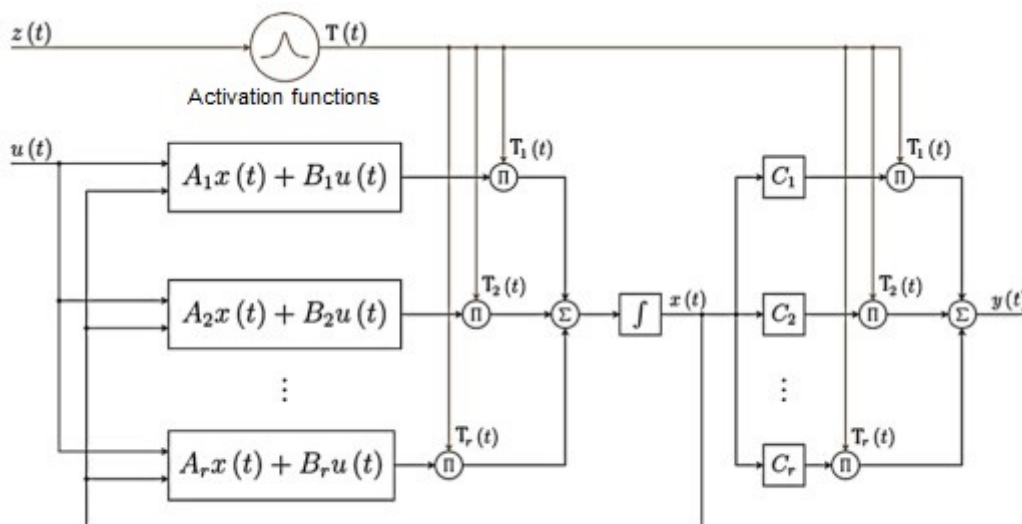
Figure 2.2: The Takagi-Sugeno fuzzy model diagram

2.3.2 Construction of a TS fuzzy model

In order to obtain a T-S model (2.2), we can mention three approaches widely used in literature. The first approach is based on identification techniques. The structure of the model as well as the activation functions are first chosen by using input-output data sets collected from measurements performed on the real system, identification techniques are

then implemented.

The second approach is based on the linearization of the nonlinear model around several operating points. Linear sub-models are then obtained for each operating zone. Using optimization techniques to minimize the squared output error, the activation functions can be generated for each operating area.

The third approach is based directly on the analytical knowledge of the nonlinear model. It is known as the nonlinear sector transformation. Unlike the two previous approaches which give an approximation of the nonlinear model, this third method provides a T-S model representing in an exact way the nonlinear model in a compact of the state space. The work presented in this thesis mainly uses the nonlinear sector approach.

2.3.2.1 The linear sector approach

This method is suited for nonlinear systems with moderate non linearities. From the mathematical model, we can obtain easily the TS model which will represent the model in an exact way without approximation in the domain of the premise variables.
This approach can be applied to mathematical models having the following form:

$$\begin{cases} \dot{x}(t) = (f(x(t)).x(t) + g(x(t)).u(t) \\ y(t) = h(x(t)).x(t) \end{cases} \tag{2.3}$$

With: f, g and h nonlinear functions.

In order to obtain the TS model, let k be the number of nonlinear functions present in the system (2.2). We note them f_i, $i = 1, ..., k$. We suppose that it exists a compact C of the variables $z(t)$ where the nonlinearities are bounded:

$$f_i \in [f_{min}^i; f_{max}^i], \quad i = 1, ..., k \tag{2.4}$$

The nonlinearities f_i can then be written as follows:

$$f_i(z(t)) = f_{min}^i.\omega_0^i(z(t)) + f_{max}^i.\omega_1^i(z(t)) \tag{2.5}$$

where:

$$\begin{cases} \omega_0^i = \frac{f_{max}^i - f_i(z(t))}{f_{max}^i - f_{min}^i} \\ \omega_1^i = \frac{f_i(z(t)) - f_{min}^i}{f_{max}^i - f_{min}^i} \end{cases} \tag{2.6}$$

which verify the following properties: $\omega_0^i \geq 0, \quad \omega_1^i \geq 0 \quad \omega_0^i + \omega_1^i = 1$

The activation functions $T_i(z(t)), i = 1, ..., r$ are obtained from the functions ω_0^i and ω_0^i by:

$$T_{1+i_1+2i_2+...+2^{k-1}i_k}(z(t)) = \prod_{j=1}^{k} \omega_{i_j}^j \tag{2.7}$$

The number of sub-models r is equal to 2^k.
And finally The rules of fuzzy models can be presented in the following form:

If $z_1(t)$ is $\omega_1^{i_1}$ and ... $z_k(t)$ is $\omega_k^{i_k}$ then:

$$\begin{cases} \dot{x}(t) = A_i x(t) + B_i u(t) \\ y(t) = C_i x(t) \end{cases} \tag{2.8}$$

knowing that: i_k are boolean values that can only take 0 or 1.

2.3.3 Example: Electric vehicle model

We remind that the nonlinear model of the electric vehicle is given by the equation (1.12) and by taking $x_1(t) = \dot{x}(t)$ and $x_2(t) = T_e(t)$:

$$\begin{cases} \dot{X}(t) = \begin{bmatrix} -\frac{a_x + b_x . x_1(t)}{\alpha} & \frac{R_{ap}}{\alpha} \\ 0 & -\frac{1}{\tau_e} \end{bmatrix} . X(t) + \begin{bmatrix} 0 \\ \frac{1}{\tau_e} \end{bmatrix} u_e \\ y = \begin{bmatrix} e + f . \dot{x}(t) & 0 \end{bmatrix} X \end{cases} \tag{2.9}$$

We apply the linear sector approach on the latter

x_1 represents the velocity of the vehicle, it is assumed that $x_1 \in [v_{min}, v_{max}]$ with $v_{min}, v_{max} > 0$ and are constants.

We can notice that there is only one non-linearity in the mathematical model that we will note f_1 where: $f_1 = x_1$

Consider the following premise vector: $z(t) = x_1(t)$
The term x_1 is within the range of $[v_{min}; v_{max}]$

Applying the equation (2.6) to this example we find:

$$\begin{cases} \omega_0^1 = \frac{f_{max}^i - f_i(z(t))}{f_{max}^i - f_{min}^i} = \frac{v_{max} - x_1}{v_{max} - v_{min}} \\ \omega_1^1 = \frac{f_i(z(t)) - f_{min}^i}{f_{max}^i - f_{min}^i} = \frac{x_1 - v_{min}}{v_{max} - v_{min}} \end{cases} \tag{2.10}$$

And by applying the equation (2.7) we find:

$$T_1 = \omega_0^1 \qquad T_2 = \omega_1^1 \tag{2.11}$$

We end up with two local models, each model corresponds to a fuzzy rule, they are constituted from the combinations of the bounds of the non linear terms such as:

Rule 1: If $x_1(t)$ is ω_0^1 then : $\begin{cases} \dot{x}(t) = A_1 x(t) + B_1 u(t) \\ y(t) = C_1 x(t) \end{cases}$

Rule 1: If $x_1(t)$ is ω_1^1 then : $\begin{cases} \dot{x}(t) = A_2 x(t) + B_2 u(t) \\ y(t) = C_2 x(t) \end{cases}$

Where the matrices A_i, B_i, C_i are obtained from the possible combinations of the bounds

of the nonlinear terms:

$$
\begin{cases}
A_1 = \begin{bmatrix} -\dfrac{a_x + b_x.v_{max}}{\alpha} & \dfrac{R_{ap}}{\alpha} \\ 0 & -\dfrac{1}{\tau_e} \end{bmatrix}, B_1 = \begin{bmatrix} 0 \\ \dfrac{1}{\tau_e} \end{bmatrix}, C_1 = \begin{bmatrix} e + f.v_{max} & 0 \end{bmatrix} \\
A_2 = \begin{bmatrix} -\dfrac{a_x + b_x.v_{min}}{\alpha} & \dfrac{R_{ap}}{\alpha} \\ 0 & -\dfrac{1}{\tau_e} \end{bmatrix}, B_2 = \begin{bmatrix} 0 \\ \dfrac{1}{\tau_e} \end{bmatrix}, C_2 = \begin{bmatrix} e + f.v_{min} & 0 \end{bmatrix}
\end{cases}
\tag{2.12}
$$

$$
A1 = \begin{bmatrix} -0.009 & 0.0183 \\ 0 & -20 \end{bmatrix} \quad B_1 = \begin{bmatrix} 0 \\ 20 \end{bmatrix}, \quad C_1 = \begin{bmatrix} 1.54 & 0 \end{bmatrix}
$$
$$
A2 = \begin{bmatrix} -0.0078 & 0.0187 \\ 0 & -20 \end{bmatrix} \quad B_2 = \begin{bmatrix} 0 \\ 20 \end{bmatrix}, \quad C_2 = \begin{bmatrix} 0.7 & 0 \end{bmatrix}
$$

2.4 Stability of TS fuzzy model

The particular structure of TS fuzzy model has allowed the extension of the study of the stability of linear systems to the case of non-linear systems.
To find if the TS model is stable or to find a stabilizing control law, we will rely on the second Lyapunov method which leads to sufficient conditions of stability.

Let be an autonomous Takagi-Sugeno system, represented by :

$$
\dot{x}(t) = \sum_{i=1}^{r} T_i(z(t)).A_i x(t) \tag{2.13}
$$

Theorem 2.1 [6] The system (2.12) is said to be quadratically stable if there exists a matrix $P \in R^{n \times n}$ symmetric and positive definite such that the following conditions are satisfied for $i = 1, ..., r$:

$$
A_i^T P + P A_i < 0 \tag{2.14}
$$

Proof. It is based on the choice of a quadratic Lyapunov function $V(x) = x(t)^T P x(t)$ with $P = P^T > 0$. The use of the convex sum property of Lyapunov functions allows to obtain r conditions, to be solved simultaneously, formulated in terms of matrix linear inequalities (LMIs).
To check the stability, we derive the Lyapunov function :

$$
\frac{d}{dt} V(x(t)) = \frac{d}{dt} x(t)^T P x(t) = \dot{x}(t)^T P x(t) + x(t)^T P \dot{x}(t) \tag{2.15}
$$

By replacing $\dot{x}$ with the fuzzy model TS (equation 2.11) :

$$
\frac{d}{dt} V(x(t)) = (\sum_{i=1}^{r} T_i(z(t)).A_i x(t))^T P x(t) + x(t)^T P \sum_{i=1}^{r} T_i(z(t)).A_i x(t)
$$

$$
= \sum_{i=1}^{r} T_i(z(t)).A_i x(t))^T P x(t) + x(t)^T P \sum_{i=1}^{r} T_i(z(t)).A_i x(t)
$$

$$= \sum_{i=1}^{r} T_i(z(t)).(A_i^T P + PA_i)x(t) \tag{2.16}$$

To prove that the model is stable, we check the inequality:

$$\frac{d}{dt}V(x(t)) < 0 \tag{2.17}$$

As consequence:

$$\sum_{i=1}^{r} T_i(z(t)).(A_i^T P + PA_i)x(t) < 0 \quad \forall i \in 1,..,r \tag{2.18}$$

Hence, the proof of the theorem. $\qquad\qquad\square$

-The sufficient conditions for stability (asymptotic convergence to the origin $x(t) = 0$ from any initial point) are given by this theorem.
-The non existence of the P matrix does not mean that the system is unstable.

2.5 Stabilization of systems described by TS models

For the stabilization of the system, we will use a nonlinear state feedback with constant gains K_i weighted by the same activation functions of the TS model. This method is called Parallel distributed compensation (PDC), and it is based upon the second method of Lyapunov.

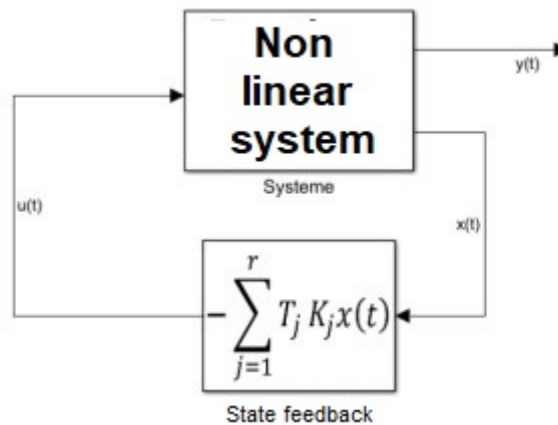Figure 2.3: PDC control diagram

The command law has the following form:

$$u(t) = -\sum_{j=1}^{r} T_j K_j x(t) \tag{2.19}$$

By substituting the equation (2.18) in (2.2) we find:

$$\dot{x}(t) = \sum_{i=1}^{r} T_i(z(t)).(A_i x(t) - B_i \sum_{j=1}^{r} T_j K_j x(t)) \tag{2.20}$$

given that: $\sum_{j=1}^{r} T_j(z(t)) = 1$ then:

$$\dot{x}(t) = \sum_{i=1}^{r} T_i(z(t)).(\sum_{j=1}^{r} T_j A_i x(t) - B_i \sum_{j=1}^{r} T_j K_j x(t))$$

$$\dot{x}(t) = \sum_{i=1}^{r} T_i(z(t)).(\sum_{j=1}^{r} T_j (A_i x(t) - T_j B_i K_j x(t)))$$

$$\dot{x}(t) = \sum_{i=1}^{r} \sum_{j=1}^{r} T_i T_j (A_i - B_i K_j) x(t) \tag{2.21}$$

We put:

$$G_{ij} = A_i - B_i K_j \tag{2.22}$$

which results in:

$$\dot{x}(t) = \sum_{i=1}^{r} \sum_{j=1}^{r} T_i T_j G_{ij} x(t) \tag{2.23}$$

Theorem 2.2 [7] The system (2.22) is said to be globally asymptotically stable if there exists a matrix $P \in R^{n \times n}$ symmetric and positive definite such that the following conditions are satisfied for $i = 1, ..., r$:

$$G_{ii}^T P + P G_{ii} < 0 \tag{2.24}$$

$$(\frac{G_{ij} + G_{ji}}{2})^T P + P(\frac{G_{ij} + G_{ji}}{2}) \leq 0 \tag{2.25}$$

But the inequalities are not linear with respect to the variables P and K_i. We make the following bijective changes of variables: $X = P^{-1}$, $N_i = K_i X$

$$G_{ii}^T X^{-1} + X^{-1} G_{ii} < 0$$

$$G_{ii}^T + X^{-1} G_{ii} X < 0$$

$$X G_{ii}^T + G_{ii} X < 0$$

$$X A_i^T - X K_i^T B_i^T + A_i X - K_i B_i X < 0$$

$$X A_i^T + A_i X - N_i^T B_i^T - B_i N_i < 0 \tag{2.26}$$

A similair development is applied to (2.24) to obtain:

$$X A_i^T + A_i X + X A_j^T + A_j X - N_i^T B_j^T - B_j N_i - N_j^T B_i^T - B_i N_j \leq 0 \tag{2.27}$$

The K_i parameters of the controller are calculated from:

$$K_i = N_i X^{-1} \tag{2.28}$$

2.5.1 Relaxation of LMIs

If the mathematical model of the system has several nonlinearities that will give 2^k local models and in the case where the matrices A,B and C are of high dimension, finding a matrix P that is solution to equations (2.23) and (2.24) is not always possible, which requires to relieve the LMIs.

Theorem 2.3 [8] The system (2.22) is said to be globally asymptotically stable if there exists matrices P and M symmetric and positive definite such that the following conditions are satisfied for $i = 1, ..., r$:

$$G_{ii}^T P + P G_{ii} + (r-1)M < 0 \tag{2.29}$$

$$(\frac{G_{ij} + G_{ji}}{2})^T P + P(\frac{G_{ij} + G_{ji}}{2}) - M < 0 \tag{2.30}$$

with r is the number of TS local models.
By applying the same bijective changes of variables: $X = P^{-1}$, $N_i = K_i X$:

$$X A_i^T + A_i X - N_i^T B_i^T - B_i N_i + (r-1)M < 0 \tag{2.31}$$

$$X A_i^T + A_i X + X A_j^T + A_j X - N_i^T B_j^T - B_j N_i - N_j^T B_i^T - B_i N_j - M \leq 0 \tag{2.32}$$

2.6 Stabilization with fuzzy observer

The state of the system is not always available, but the synthesis of the PDC control law which is a state feedback formed by a combination of gains weighted by activation functions requires its knowledge. Therefore we must use an observer that will estimate it. In the case of TS models, we prefer TS fuzzy observers (generally based on linear models) of the "Luenberger" type. The latter, have the advantage of having the same structure as the TS models.
The structure of a TS fuzzy observer is obtained by combining r local Luenberger observers. It is described by the following form following :

$$\begin{cases} \dot{\hat{x}}(t) = \sum_{i=1}^r T_i(\hat{z}(t)).(A_i\hat{x}(t) + B_i u(t) + L_i(y(t) - \hat{y}(t)) \\ \hat{y}(t) = \sum_{i=1}^r T_i(\hat{z}(t)).(C_i\hat{x}(t)) \end{cases} \tag{2.33}$$

With: $\hat{x}(t)$ is the estimated (observed) state vector, $\hat{z}(t)$ is the vector of premises reconstructed, and L_i are the gains of the Luenberger observer.
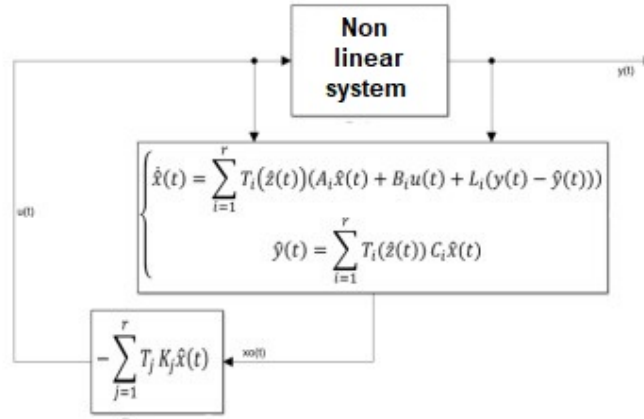
Figure 2.4: Diagram of the PDC control and states observed by a fuzzy observer

Hypothesis: we will suppose that the variables of the premises are available ($\hat{z}(t) = z(t)$) and therefore the activation functions of the observer and the system are identical:

$$T_i(\hat{z}(t)) = T_i(z(t)) \tag{2.34}$$

In order to define the convergence of the estimated values to the exact values we take :

$$e(t) = x(t) - \hat{x}(t) \tag{2.35}$$

We derive:

$$\dot{e}(t) = \dot{x}(t) - \dot{\hat{x}}(t) \tag{2.36}$$

Substituting equations (2.2) and (2.32) in equation (2.35):

$$\dot{e}(t) = \sum_{i=1}^{r} T_i(z(t)).(A_i x(t) + B_i u(t)) - \sum_{i=1}^{r} T_i(\hat{z}(t)).(A_i \hat{x}(t) + B_i u(t) + L_i(y(t) - \hat{y}(t)) \tag{2.37}$$

Using equation (2.33) in (2.36) we find:

$$\dot{e}(t) = \sum_{i=1}^{r} T_i(z(t)).((A_i x(t) + B_i u(t)) - (A_i \hat{x}(t) + B_i u(t) + L_i(y(t) - \hat{y}(t))) \tag{2.38}$$

$$\dot{e}(t) = \sum_{i=1}^{r} T_i(z(t)).(A_i(x(t) - \hat{x}(t)) - L_i(y(t) - \hat{y}(t)) \tag{2.39}$$

By substituting the expressions of $y(t)$ and $\hat{y}(t)$ (equations (2.2) and (2.32)) in equation (2.38):

$$\dot{e}(t) = \sum_{i=1}^{r} T_i(z(t)).(A_i(x(t) - \hat{x}(t)) - L_i(\sum_{j=1}^{r} T_j(z(t)).(C_j x(t)) - \sum_{j=1}^{r} T_j(z(t)).(C_j \hat{x}(t)))$$
$$\tag{2.40}$$

Since $\sum_{i=1}^{r} T_j(z(t))$:

$$\dot{e}(t) = \sum_{i=1}^{r} T_i(z(t)).(A_i \sum_{i=1}^{r} T_j(z(t))(x(t) - \hat{x}(t)) - L_i(\sum_{j=1}^{r} T_j(z(t)).(C_j x(t)) - \sum_{i=1}^{r} T_j(z(t)).(C_j \hat{x}(t)))$$

$$\dot{e}(t) = \sum_{i=1}^{r} (A_i(x(t) - \hat{x}(t)) - L_iC_j(x(t) - \hat{x}(t)))$$

$$\dot{e}(t) = \sum_{i=1}^{r} T_iT_j(A_i - L_iC_j)e(t) \tag{2.41}$$

We put:

$$O_{ij} = A_i - L_iC_j \tag{2.42}$$

Then:

$$\dot{e}(t) = \sum_{i=1}^{r} T_iT_jO_{ij}e(t) \tag{2.43}$$

The gains L_i are chosen to ensure the convergence of the estimated values to the actual values (convergence of the error to the origin).

The PDC control law is synthesized based on the estimated values of the state by the observer:

$$u(t) = -\sum_{j=1}^{r} T_jK_j\hat{x}(t) \tag{2.44}$$

By substituting the equation (2.43) in (2.2) we find:

$$\dot{x}(t) = \sum_{i=1}^{r} T_i(z(t)).(A_ix(t) - B_i\sum_{j=1}^{r} T_jK_j\hat{x}(t)) \tag{2.45}$$

Using equation (2.34) we have

$$\hat{x}(t) = x(t) - e(t) \tag{2.46}$$

By substituting the equation (2.45) in (2.44) we find:

$$\dot{x}(t) = \sum_{i=1}^{r} T_i(z(t)).(A_ix(t) - B_i\sum_{j=1}^{r} T_jK_j(x(t) - e(t)))$$

$$\dot{x}(t) = \sum_{i=1}^{r}(\sum_{j=1}^{r} T_iT_jG_{ij}x(t) + B_iK_je(t)) \tag{2.47}$$

By combining the two models (2.42) and (2.46) we obtain the augmented system:

$$\begin{cases} \dot{x}(t) = \sum_{i=1}^{r}(\sum_{j=1}^{r} T_iT_jG_{ij}x(t) + B_iK_je(t)) \\ \dot{e}(t) = \sum_{i=1}^{r} T_iT_jO_{ij}e(t) \end{cases} \tag{2.48}$$

Taking the following augmented state vector:

$$X = \begin{bmatrix} x \\ e \end{bmatrix} \tag{2.49}$$

We find:

$$\dot{X}(t) = \sum_{i=1}^{r} T_iT_jM_{ij}X(t) \tag{2.50}$$

With:

$$M_{ij} = \begin{bmatrix} G_{ij} & B_i K_j \\ 0 & O_{ij} \end{bmatrix} \tag{2.51}$$

In the case of linear systems, we apply the separation technique to solve such a problem. For TS fuzzy models this property is valid in the case where the variables of the premises are measurable which is assumed at the beginning.

$$\begin{cases} G_{ii}^T P + P G_{ii} + (r-1)M < 0 & i = 1, .., r \\ (\frac{G_{ij}+G_{ji}}{2})^T P + P(\frac{G_{ij}+G_{ji}}{2}) - M < 0 & i < j \end{cases} \tag{2.52}$$

$$\begin{cases} Oii^T P + P O_{ii} + (r-1)M < 0 & i = 1, .., r \\ (\frac{O_{ij}+O_{ji}}{2})^T P + P(\frac{O_{ij}+O_{ji}}{2}) - M < 0 & i < j \end{cases} \tag{2.53}$$

We end up with inequalities similar to those already found in chapter 2, as far as stability is concerned, we find the same LMIs (2.30) and (2.31):

$$\begin{cases} X A_i^T + A_i X - N_i^T B_i^T - B_i N_i + (r-1)M < 0 & i = 1, .., r \\ X A_i^T + A_i X + X A_j^T + A_j X - N_i^T B_j^T - B_j N_i - N_j^T B_i^T - B_i N_j - M \leq 0 & i < j \end{cases} \tag{2.54}$$

For that of the observer, we must make a single change of variable. We replace the matrix $O_i i$ by its expression (2.41). and we pose that $N_i = P L_i$:

$$\begin{cases} A_i^T P + P A_i - C_i^T N_i^T - N_i C_i + (r-1)M < 0 & i = 1, .., r \\ A_i^T P + P A_i + A_j^T P + P A_j - C_i^T N_j^T - N_j C_i - C_j^T N_i^T - N_i C_j - M \leq 0 & i < j \end{cases} \tag{2.55}$$

2.7   Stabilization with integral action

v!   As in the case of a linear system model, the addition of an integral action allows to have a static error of zero, this is already used with a PDC command to synthesize a stabilizing control law and ensure the tracking of the set point at the same time.
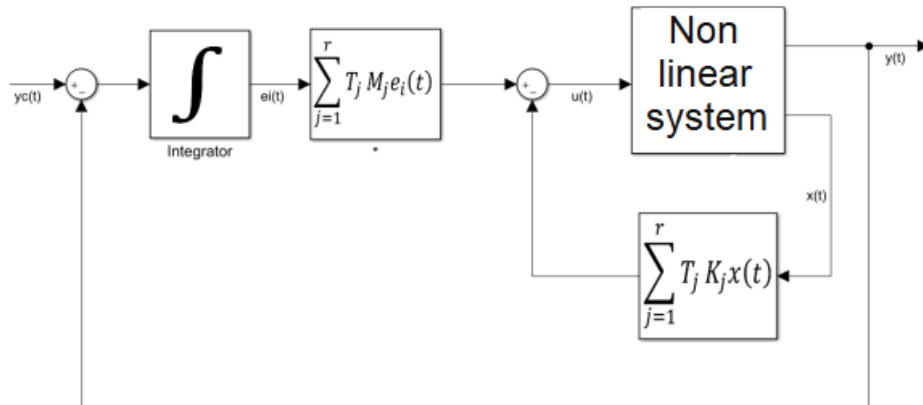

Figure 2.5: Control diagram with integral structure

This control structure ensures the convergence of the error $e(t)$ to the origin which allows the tracking of the set point. We will use the same method in order to stabilize the TS fuzzy system model, we just need to rewrite the model by increasing the state. From the figure 2.5, we can write:

$$\dot{E} = y_c - y \tag{2.56}$$

We consider the augmented state:

$$X = \begin{bmatrix} x \\ E \end{bmatrix} \tag{2.57}$$

Equations (2.2) and (2.55) in (2.56) gives the following model:

$$\dot{X} = \begin{bmatrix} \dot{x} \\ \dot{E} \end{bmatrix} = \begin{bmatrix} \sum_{i=1}^{r} T_i(z(t)).(A_i x(t) + B_i u(t)) \\ y_c - y \end{bmatrix} \tag{2.58}$$

We replace the output $y(t)$ withh its expression :

$$\dot{X} = \begin{bmatrix} \dot{x} \\ \dot{E} \end{bmatrix} = \begin{bmatrix} \sum_{i=1}^{r} T_i(z(t)).(A_i x(t) + B_i u(t)) \\ y_c - \sum_{i=1}^{r} T_i(z(t)).(C_i x(t)) \end{bmatrix} \tag{2.59}$$

Knowing that $\sum_{i=1}^{r} T_i(z(t))$ and y_c is not dependent on i:

$$\dot{X} = \begin{bmatrix} \dot{x} \\ \dot{E} \end{bmatrix} = \begin{bmatrix} \sum_{i=1}^{r} T_i(z(t)).(A_i x(t) + B_i u(t)) \\ \sum_{i=1}^{r} T_i(z(t)).y_c - \sum_{i=1}^{r} T_i(z(t)).(C_i x(t)) \end{bmatrix}$$

$$\dot{X} = \begin{bmatrix} \dot{x} \\ \dot{E} \end{bmatrix} = \begin{bmatrix} \sum_{i=1}^{r} T_i(z(t)).(A_i x(t) + B_i u(t)) \\ \sum_{i=1}^{r} T_i(z(t)).(y_c - C_i x(t)) \end{bmatrix} \tag{2.60}$$

$$\dot{X} = \sum_{i=1}^{r} T_i(z(t))(\begin{bmatrix} I \\ 0 \end{bmatrix} (A_i x(t) + B_i u(t)) + \begin{bmatrix} 0 \\ I \end{bmatrix} (y_c - C_i x(t)))$$

$$\dot{X} = \sum_{i=1}^{r} T_i(z(t))(\begin{bmatrix} A_i \\ 0 \end{bmatrix} x(t) + \begin{bmatrix} B_i \\ 0 \end{bmatrix} u(t)) + \begin{bmatrix} 0 \\ I \end{bmatrix} y_c - \begin{bmatrix} 0 \\ C_i \end{bmatrix} x(t))$$

$$\dot{X} = \sum_{i=1}^{r} T_i(z(t))(\begin{bmatrix} A_i \\ -C_i \end{bmatrix} x(t) + \begin{bmatrix} B_i \\ 0 \end{bmatrix} u(t)) + \begin{bmatrix} 0 \\ I \end{bmatrix} y_c + \begin{bmatrix} 0 \\ 0 \end{bmatrix} E(t))$$

$$\dot{X} = \sum_{i=1}^{r} T_i(z(t))(\begin{bmatrix} A_i & 0 \\ -C_i & 0 \end{bmatrix} X(t) + \begin{bmatrix} B_i \\ 0 \end{bmatrix} u(t)) + \begin{bmatrix} 0 \\ I \end{bmatrix} y_c) \tag{2.61}$$

We put; $\overline{A_i} = \begin{bmatrix} A_i & 0 \\ -C_i & 0 \end{bmatrix}$, $\overline{B_i} = \begin{bmatrix} B_i \\ 0 \end{bmatrix}$, $\overline{B_c} = \begin{bmatrix} 0 \\ I \end{bmatrix}$

This gives the augmented state model:

$$\dot{X} = \sum_{i=1}^{r} T_i(z(t))(\overline{A_i} X(t) + \overline{B_i} u(t)) + \overline{B_c} y_c) \tag{2.62}$$

The PDC control law is applied to the augmented model:

$$u(t) = - \sum_{i=1}^{r} T_j \overline{K_j} X(t) \tag{2.63}$$

with:

$$\overline{K_j} = \begin{bmatrix} K_j & -M \end{bmatrix} \tag{2.64}$$

To calculate the $\overline{K_j}$, it is sufficient to solve the following inequalities:

$$X\overline{A_i}^T + \overline{A_i}X - N_i^T\overline{B_i}^T - \overline{B_i}N_i + (r-1)M < 0 \tag{2.65}$$

$$X\overline{A_i}^T + \overline{A_i}X + X\overline{A_j}^T + \overline{A_j}X - N_i^T\overline{B_j}^T - \overline{B_j}N_i - N_j^T\overline{B_i}^T - \overline{B_i}N_j - M \leq 0 \tag{2.66}$$

Note

We can combine the usage of the observer to estimate the state that will be used to synthesize the PDC control law and the integral structure that allows tracking the set point.
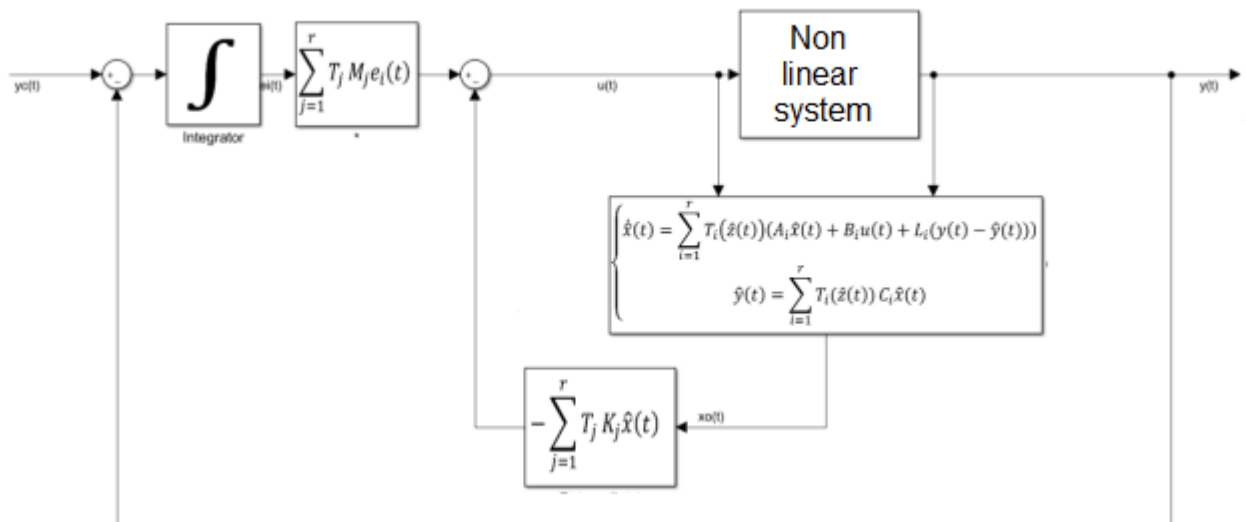
Figure 2.6: Control diagram with integral structure and fuzzy observer

2.8 Performance improvement

2.8.1 Decay rate

The theorems already seen only guarantee the global stability of the fuzzy model of Takagi-Sugeno. To ensure that the system response is faster and more performant, additional constraints involving the dominant terms G_{ii} and G_{ij} have been proposed. Thereafter, the rate of decay is guaranteed by shifting the problem only to the more naturally controllable dominant terms, moreover, the idea of relaxing the constraints at the level of the crossed terms is maintained.

Theorem 2.4 [8] If there exist symmetric matrices $P > 0$ and $M \geq 0$, matrices K_i

and a scalar α that verify:

$$G_{ii}^T P + P G_{ii} + (r-1)M + 2\alpha r P < 0 \tag{2.67}$$

$$(\frac{G_{ij} + G_{ji}}{2})^T P + P(\frac{G_{ij} + G_{ji}}{2}) - M < 0 \tag{2.68}$$

With : $G_{ij} = A_i - B_i K_j$ and r being the number of local models, then the Takagi-Sugeno multi-model is globally exponentially stable with a decay velocity at least equal to α.

To implement the method, we have to go through changes of variables $X = P^{-1}, N_i = K_i X$ and $Y = XMX$ which gives:

$$XA_i^T + A_i X - N_i^T B_i^T - B_i N_i + (r-1)Y + 2\alpha r X < 0 \ \ i \in \{1,..,r\} \tag{2.69}$$

$$XA_i^T + A_i X + XA_j^T + A_j X - N_i^T B_j^T - B_j N_i - N_j^T B_i^T - B_i N_j - 2Y \leq 0 \ \ i < j \tag{2.70}$$

2.8.2 Pole placement in LMI regions

2.8.2.1 Introduction

The temporal response of a linear system is related to the location of the poles of its transfer function in the complex plane and, in the case of Takagi-Sugeno systems Takagi-Sugeno systems, the response depends on the location of the poles of the sub-models. Indeed, the real parts of the poles have an effect on the velocity of convergence speed of the associated modes. The imaginary parts, on the other hand influence the presence of oscillations and overshoots as well as the response time response time at 5%. Therefore, one of the techniques to improve the performance of a the performance of a control law or an observer is to place the poles of the the poles of the loop system or the observer in regions of the complex plane with certain interesting properties. These regions are called LMI regions.

2.8.2.2 Definition of an LMI region

A region S of the complex plane is called an LMI region if there exists a symmetric matrix $A \in R^{n \times n}$ and a matrix $B \in R^{n \times n}$ such that:

$$S = \{z \in C : f(z) < 0\}$$

with: $f(z) = A + zB + \overline{z}B^T$ where $f(z)$ is called the characteristic function of S and $\overline{z}$ is the conjugate of z.
The LMI regions are a surface of the complex plane that depends on z and $\overline{z}$ (or on the real and imaginary part of z)

$$Re(z) = \frac{z + \overline{z}}{2} \tag{2.71}$$

$$Im(z) = \frac{z - \overline{z}}{2j} \tag{2.72}$$

2.8.2.3 Example of some interesting LMI regions

Region 1:

The left plane where the poles are with negative real part can be written :

$$\text{Re(z)}<0$$

$$\frac{z+\overline{z}}{2} < 0; z + \overline{z} < 0 \text{ with A=0 and B=1}$$

We can consider another more generalized region where :

$$Re(z) \leq -\lambda; \lambda \geq 0 \tag{2.73}$$

The characteristic equation of this region is given by:

$$f_1(z) = z + \overline{z} + 2\lambda < 0 \tag{2.74}$$

This region can be used to have faster systems by increasing the state convergence velocity of the system. By changing λ one plays on the time response time and thus ensure stability (called α-stability).
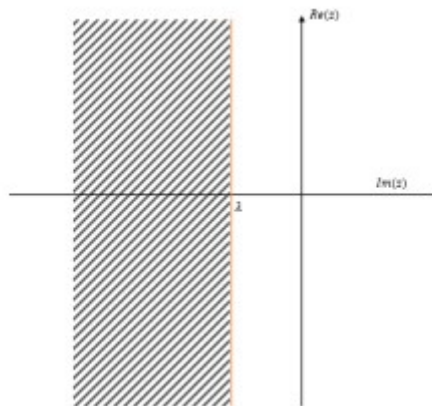
Figure 2.7: LMI region 1

Region 2:

The disk centered at the origin of the complex plane of radius r .Using the expression of the modulus :

$$\overline{z}z < r^2 \tag{2.75}$$

Using Schur's complement:

$$f_2(z) = \begin{bmatrix} -r & z \\ \overline{z} & -r \end{bmatrix} \tag{2.76}$$

This region can be used to limit the fastest dynamics by changing the radius r.
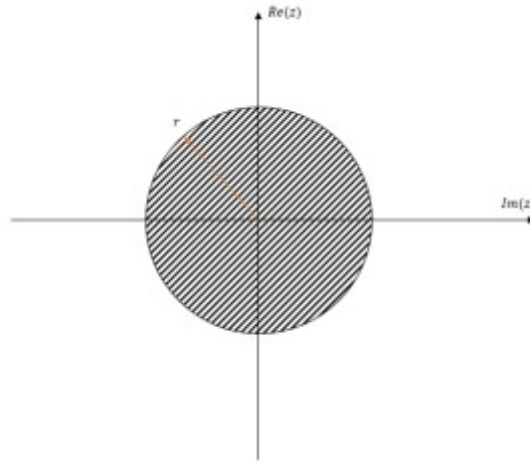
Figure 2.8: LMI region 2

Region 3:

The cone coming from the origin and of angle 2θ :

$$Re(z)tan(\theta) < -|Im(z)| \tag{2.77}$$

Using Schur's complement:

$$f_3(z) = \begin{bmatrix} (z + \overline{z})sin(\theta) & (z - \overline{z})cos(\theta) \\ (\overline{z} - z)cos(\theta) & (z + \overline{z})sin(\theta) \end{bmatrix} \tag{2.78}$$

This region affects the damping of the time response by changing the angle θ.
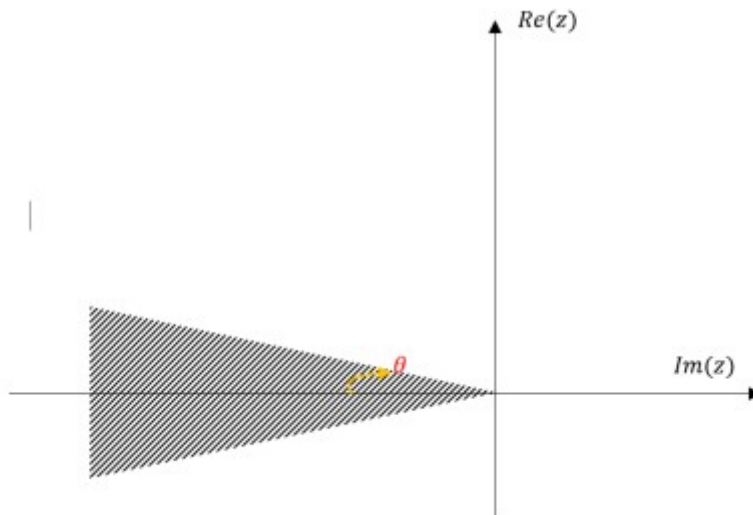
Figure 2.9: LMI region 3

2.8.2.4 Conditions for placing poles in LMI regions

Theorem 2.5 [9] The eigenvalues of a real matrix M are placed in an LMI region S of the complex plane if, and only if, there exists a symmetric matrix P such that:

$$A \otimes P + B \otimes MP + B^T \otimes PM^T < 0 \tag{2.79}$$

with: $\otimes$ Kronecker's matrix product.

Note: we find the LMI by making the following substitution :

$$(1, z, \overline{z}) \leftrightarrow (P, MP, PM^T)$$

The result is applied for the mentioned regions:

Region 1:

$$\exists P > 0 : MP + PM^T + 2\lambda P < 0 \tag{2.80}$$

Region 2:

$$\exists P > 0 : \begin{bmatrix} -rP & MP \\ PM^T & -rP \end{bmatrix} < 0 \tag{2.81}$$

Region 3:

$$\exists P > 0 : \begin{bmatrix} (MP + PM^T)sin(\theta) & (MP - PM^T)cos(\theta) \\ (PM^T - MP)cos(\theta) & (MP + PM^T)sin(\theta) \end{bmatrix} < 0 \tag{2.82}$$

Theorem 2.6 [10] Let be two LMI regions S_1 and S_2 of the complex plane. The eigenvalues of the matrix M are all in the LMI region $S_1 \cup S_2$ if and only if there exists a symmetric matrix $X > 0$ solution of the system :

$$\begin{cases} A_1 \otimes P + B_1 \otimes MP + B_1^T \otimes PM^T < 0 \\ A_2 \otimes P + B_2 \otimes MP + B_2^T \otimes PM^T < 0 \end{cases} \tag{2.83}$$

So, we can use the intersection of the 3 regions so that we can put the poles of the matrix A ($\dot{x} = Ax$) in the desired area.
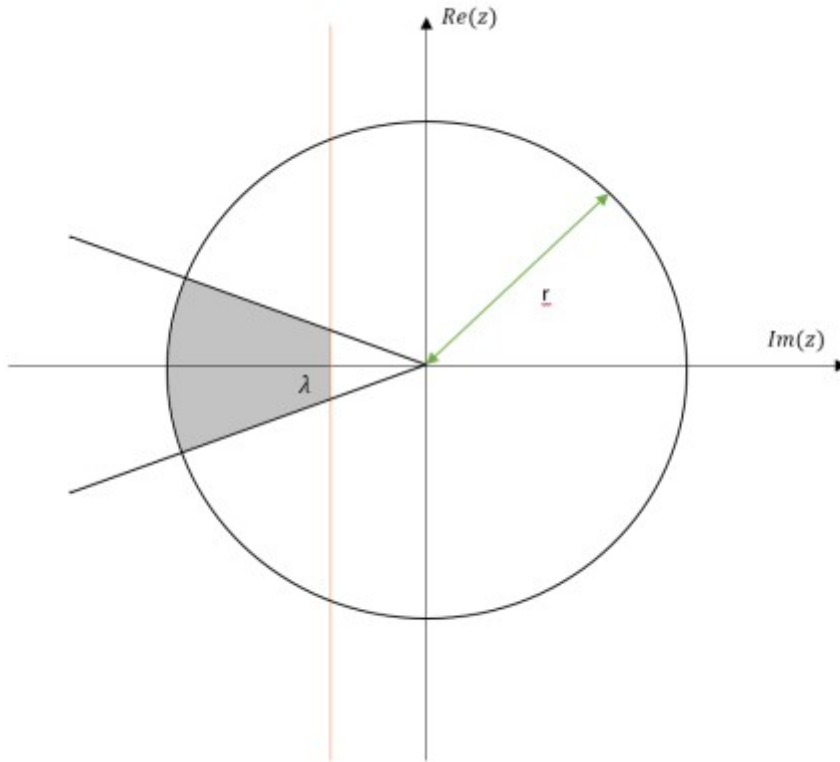
Figure 2.10: Intersection of three LMI regions

Note:

In the case where the measurement is unavailable, we must synthesize an observer to estimate the state, this observer must be faster than the system and limit the reconstruction of the measurement noise. In this case we must limit the real parts of the poles of the observer by imposing them in a vertical band with the characteristic function is given:

$$f_2(z) = \begin{bmatrix} -2_{max} + \overline{z} + z & 0 \\ 0 & 2_{min} - (\overline{z} + z) \end{bmatrix} \tag{2.84}$$

This gives the following inequality :

$$\exists P > 0 : \begin{bmatrix} -2_{max} + MP + PM^T & 0 \\ 0 & 2_{min} - (MP + PM^T) \end{bmatrix} < 0 \tag{2.85}$$

2.8.2.5 Placement of poles in LMI regions for fuzzy model of takagi sugeno

The model is described in the equation 2.21
The system and the closed loop matrix are given by the equations 2.23 and 2.22
For the matrix A_{BF} to be in an LMI region it is sufficient that:

Region 1:

$$(\sum_{i=1}^{r} \sum_{j=1}^{r} T_i T_j G_{ij} x(t))P + P(\sum_{i=1}^{r} \sum_{j=1}^{r} T_i T_j G_{ij} x(t))^T + 2\lambda P < 0 \tag{2.86}$$

This gives the following conditions:

$$G_{ii}P + PG_{ii}^T + 2\lambda P < 0, i \in \{1, .., r\}$$

$$(\frac{G_{ij} + G_{ji}}{2})P + P(\frac{G_{ij} + G_{ji}}{2})^T + 2\lambda P \le 0, i < j$$

Which are simply the same conditions but not relaxed from the decay rate method. Note that this expression is interpreted as a stability condition with decay rate for TS fuzzy models.

Region 2:

$$\begin{bmatrix} -rP & (\sum_{i=1}^{r} \sum_{j=1}^{r} T_i T_j G_{ij} x(t))P \\ P(\sum_{i=1}^{r} \sum_{j=1}^{r} T_i T_j G_{ij} x(t))^T & -rP \end{bmatrix} < 0 \tag{2.87}$$

This gives the following conditions:

$$\begin{bmatrix} -rP & G_{ii}P \\ PG_{ii}^T & -rP \end{bmatrix} < 0, i \in \{1, .., r\} \tag{2.88}$$

$$\begin{bmatrix} -rP & G_{ij}P \\ PG_{ij}^T & -rP \end{bmatrix} + \begin{bmatrix} -rP & G_{ji}P \\ PG_{ji}^T & -rP \end{bmatrix} < 0, i < j$$

$$\begin{bmatrix} -2rP & (G_{ij} + G_{ji})P \\ P(G_{ij} + G_{ji})^T & -2rP \end{bmatrix} \tag{2.89}$$

Region 3:

$$\begin{bmatrix} M_{11} & M_{12} \\ M_{21} & M_{22} \end{bmatrix}$$

with:

$$\begin{cases} M_{11} = M_{22} = ((\sum_{i=1}^{r} \sum_{j=1}^{r} T_i T_j G_{ii})P + P(\sum_{i=1}^{r} \sum_{j=1}^{r} T_i T_j G_{ii})^T)sin(\theta) \\ M_{12} = ((\sum_{i=1}^{r} \sum_{j=1}^{r} T_i T_j G_{ii})P - P(\sum_{i=1}^{r} \sum_{j=1}^{r} T_i T_j G_{ii})^T)cos(\theta) \\ M_{21} = (P(\sum_{i=1}^{r} \sum_{j=1}^{r} T_i T_j G_{ij})^T - (\sum_{i=1}^{r} \sum_{j=1}^{r} T_i T_j G_{ii})P+)cos(\theta) \end{cases} \tag{2.90}$$

This gives the following conditions :

$$\begin{bmatrix} (G_{ii}P + PG_{ii}^T)sin(\theta) & (G_{ii}P - PG_{ii}^T)cos(\theta) \\ (PG_{ii}^T - G_{ii}P)cos(\theta) & (G_{ii}P + PG_{ii}^T)sin(\theta) \end{bmatrix} < 0, i \in \{1, .., r\} \tag{2.91}$$

$$\begin{bmatrix} ((G_{ij} + G_{ji})P + P(G_{ij} + G_{ji})^T)sin(\theta) & ((G_{ij} + G_{ji})P - P(G_{ij} + G_{ji})^T)cos(\theta) \\ (P(G_{ij} + G_{ji})^T - (G_{ij} + G_{ji})P)cos(\theta) & ((G_{ij} + G_{ji})P + P(G_{ij} + G_{ji})^T)sin(\theta) \end{bmatrix} < 0, i < j \tag{2.92}$$

As it was done in the stabilization part, we make the matrix inequalities linear by changing the variables: $N_i = K_i P$:

Region 1:

$$\begin{cases} A_i P + P A_i^T - N_i^T B_i^T - B_i N_i + 2\lambda P < 0, i \in \{1,..,r\} \\ A_i P + P A_i^T + A_j P + P A_j^T - N_j^T B_i^T - B_i N_j - N_i^T B_j^T - B_j N_i + 4\lambda P < 0, i < j \end{cases}$$

$$(2.93)$$

Region 2:

$$\begin{cases} \begin{bmatrix} -rP & A_i P - B_i N_i \\ P A_i^T - N_i^T B_i^T & -rP \end{bmatrix} < 0, i \in \{1,..,r\} \\ \begin{bmatrix} -2rP & A_i P - B_i N_j + A_j P - B_j N_i \\ P A_i^T - N_j^T B_i^T + P A_j^T - N_i^T B_j^T & -2rP \end{bmatrix} < 0, i < j \end{cases}$$

$$(2.94)$$

Region 3:

$$\begin{cases} \begin{bmatrix} (A_i P - B_i N_i + P A_i^T - N_i^T B_i^T)sin(\theta) & (A_i P - B_i N_i - P A_i^T + N_i^T B_i^T)cos(\theta) \\ (-A_i P + B_i N_i + P A_i^T - N_i^T B_i^T)cos(\theta) & (A_i P - B_i N_i + P A_i^T - N_i^T B_i^T)sin(\theta) \end{bmatrix} < 0, i \in \{1,..,r\} \\ \begin{bmatrix} J_{11} & J_{12} \\ J_{21} & J_{22} \end{bmatrix} < 0, i < j \\ J_{11} = J_{22} = ((A_i P - B_i N_j - P A_i^T + N_j^T B_i^T) + (A_j P - B_j N_i - P A_j^T + N_i^T B_j^T))sin(\theta) \\ J_{12} = ((A_i P - B_i N_j - P A_i^T + N_j^T B_i^T) + (A_j P - B_j N_i - P A_j^T + N_i^T B_j^T))cos(\theta) \\ J_{21} = ((-A_i P + B_i N_j + P A_i^T - N_j^T B_i^T) + (-A_j P + B_j N_i + P A_j^T - N_i^T B_j^T))cos(\theta) \end{cases}$$

$$(2.95)$$

2.9   Conclusion

In this chapter, we have presented the method of nonlinear sectors which is used to represent the nonlinear system in the Takagi-Sugeno fuzzy form.

Then we analyzed the stability of such a system and we presented the PDC method which allows to stabilize the Takagi-Sugeno fuzzy systems with and without using LMI relaxation.

After that, we have presented sufficient conditions to synthesize a fuzzy observer, then we have given those which allow the trajectory tracking.

Finally, we used the decay rate to improve the convergence conditions and we presented the LMI regions for making the desired pole placement in order to locate the poles of Takagi-Sugeno models in regions that provide the stability and the desired performances in closed loop.

Chapter 3

Fault tolerant control

3.1   Introduction

Automated systems are based on various control techniques in order to perform specific missions and tasks while reaching more or less high levels of performance and safety, which are qualified as satisfactory in the nominal case. On the other hand, when a fault occurs, it can influence these performances and the whole system, causing undesired situations characterized by a degradation in the quality of the system operation or in a more serious case causing instability. The classical control methods are limited in some of these cases, they do not have the necessary options and qualities to overcome such a problem, to confront this type of problems and avoid these consequences, often we rely on the principle of hardware redundancy especially in the case of critical systems such as nuclear, aeronautical and space, despite the apparent effectiveness of this attempt, it has two main disadvantages: economic and technical, in fact, it is expensive from the point of view of cost and maintenance, as well as the physical size because of the duplication of hardware components. An alternative that can be effective and that can be used to avoid such drawbacks is based on the principle of analytical redundancy. The latter proposes to develop more sophisticated strategies that allow the system to have the ability and possibility to automatically accommodate the defects in question. Such a system is called a fault tolerant system. The fault diagnosis techniques presented are necessary and used in this context, however, these techniques are considered in most cases as an open loop monitoring tool only, Hence the need to integrate the control part and to develop techniques for fault tolerant control.

The main idea behind fault-tolerant control is to try to combine fault diagnosis and control techniques, with the objective of maintaining system stability and a certain degree of nominal performance, despite the occurrence of faults, by limiting their effect on the system or even cancelling them in a more ideal case.

This chapter is devoted to present the different concepts that concern the fault tolerance, we will classify its approaches and explain the principle of each class, we are mainly interested in the sensor faults, then, we study the effect of the faults on the system, their estimation and their compensation.

3.2   Definitions and generalities

Let's start by clarifying the definitions of a few concepts specific to diagnosis:

Defect, fault: unacceptable deviation of at least one characteristic of a system from its nominal value. It is noted $f(t) \in R^{n_f}$.

Failure: permanent interruption of the system's ability to perform its mission under specified operational conditions.

Breakdown: state of a system unable to perform its function due to a failure.

Residues: signal designed as an indicator of functional or behavioral abnormality. It is noted $r(t) \in R^{n_r}$.

Fault detection (FD): function consisting in determining the appearance and the time of occurrence of a fault. This function can be obtained by using the residue $r(t)$ generated by comparing the behavior of the system model to that of the real system. Ideally, a residue is zero when the system is in normal operation.

In observer-based diagnostic methods, generally, the residue r(t) is formed by the comparison of the estimated and measured estimated outputs and measured outputs:

$$r(t) = y(t) - \hat{y}(t) \tag{3.1}$$

In real situations, the residue $r(t)$, in the absence of a fault, has a zero mean due to the presence of noise, disturbances and modeling uncertainties in addition to the noise generated by the measurement and data acquisition chain. In the presence of faults, a deviation of the residue $r(t)$ is observed corresponding to the appearance of a fault. In order to detect a fault, the residue $r(t)$ is compared to a threshold J_t defined according to the errors of model errors, disturbances and measurement noises:

$$\begin{cases} r(t) < J_t, & \text{no fault detected} \\ r(t) \geq J_t, & \text{presence of fault} \end{cases} \tag{3.2}$$

Fault Isolation (FI): After a fault has been detected in the system, it is important to be able to locate the exact component affected. This step is called fault location or isolation. It is often based on the generation of residues so that a set of these residues is sensitive to some faults and insensitive to others. The generation of sensitive residues to combinations of faults and an adapted decision logic, allows to localize the faults.

Fault estimation or Fault identification: the estimation of the faults consists in providing at each moment the value of the fault :

$$r_i(t) = f_i(t), \quad \forall t, \quad i = 1, ..., n_r \tag{3.3}$$

In fault tolerant control problems, it is often necessary to know the magnitude and shape of the fault in order to better compensate for it. Fault estimation becomes an important problem to solve. Moreover, the estimation implies detection and localization because the estimated faults constitute residues.

3.3 Fault and modeling

The faults affecting a system can be of different natures and are generally classified into classified into actuator faults, sensor faults and system faults:

Actuator fault : An actuator fault is a failure representing a total or partial loss of an actuator leading to the loss of a control action on the system. For example, a blocked cylinder no longer responds to the control signal applied to it; this is referred to as a total

loss of the actuator. A partial fault in the actuator can be the consequence of a decrease in efficiency due to a hydraulic problem (leakage), ageing or saturation. Such faults lead to a degraded operation of the system and can even lead to its instability. The idea of using several actuators in order to prevent the consequences of an actuator fault is not always satisfactory because it leads to an increase in costs, hence the interest of fault tolerant control that we will study later.

Sensor fault : A sensor fault, which represents an error in the measurement of a physical quantity, can be partial or total. The total loss of a sensor (blockage) is due, for example, to a loss of physical connection (electrical for example) between the source of information and the sensor or a malfunction of the sensor (mechanical wear, software problem, etc..). A partial fault appears as a bias, a drift, a decrease in efficiency, a calibration fault... In order to detect sensor faults, the use of hardware redundancy is possible. This technique is very reliable, but its major drawback is the cost and the size of the system.

System fault : System faults are any faults that affect the components of the system except actuators and sensors. They reflect a change in the system parameters, e.g. mass, aerodynamic coefficients, etc. This type of fault is difficult to diagnose because of the diversity of failure situations.

The faults are also classified into additive and multiplicative faults. Often, multiplicative faults are transformed into additive faults. The design of fault diagnostic systems is easier using additive faults because they are represented by external signals and not by changes in the matrices of the system as it is the case of multiplicative faults.

3.4 Fault diagnosis

Mainly, there are two main classes of diagnostic methods: with and without mathematical model, the first class assumes the non-availability of an analytical model of the system, several methods and techniques are used, such as hardware redundancy which consists in multiplying the instruments and components, in the case of sensors for example, to make the detection, at least two sensors are needed, the localization is made only with three or more, this method is used especially in critical systems such as nuclear systems and aerospace systems Another approach without model is based on logical reasoning to build a fault tree and a decision tree. Thus, we find methods based on signal based methods that rely on input-output data analysis.

The second class contains the model-based methods, which are based on the principle of analytical redundancy of information. There are several approaches exploiting this principle, such as parametric estimation, parity space or methods based on state or output observers. The latter is the most studied and known, and it is to which we are interested in our work. We speak of observers especially in the deterministic case, in the stochastic case we speak rather of filter.

3.4.1 The concepts of observability and estimation

The estimate of the fault is the final result of its diagnosis. In this thesis, we are interested in the observer-based method.

In the framework of diagnosis, we consider a dynamic system which undergoes faults or other unknown inputs, the idea is to try to estimate both the state of the system and the unknown input, in other words, we can do what we call the reconstruction of state from the given quantities as inputs and outputs.

Among the first tools developed in this context, we find the Luenberger observer in the deterministic case and the Kalman filter in the stochastic case.Several techniques for the computation of observer gains are proposed, we cite as examples the adaptive observers, the sliding mode observers and the unknown input observers which have known a lot of interest, in particular the PI and PMI observers, which allow the simultaneous estimation of the state and the unknown inputs.

The diagnosis based on an observer with unknown inputs consists in estimating the system from a correct operation model, the estimation error between the estimated values and the measured values indicates a possible fault, residues are generated from this error, we say that a fault has been detected when the residue is far from being zero, A single observer is sufficient to carry out this detection, moreover, its localization requires more than one observer, one speaks about bank of observers which generate the whole of the various residues, which will be analyzed by using a certain logic of decision, allowing the determination of the part of the system affected by the fault in question, its localization is thus, a result of this analysis.

However, there are different architectures for building a bank of observers: the GOS (Generalized Observer Scheme) architecture, and the DOS (Dedicated Observer Scheme) architecture which are shown in the following figures (3.1) and (3.2):

In a dedicated observer bank for actuator faults with the DOS structure, the ith observer is driven by the outputs and only the ith input.
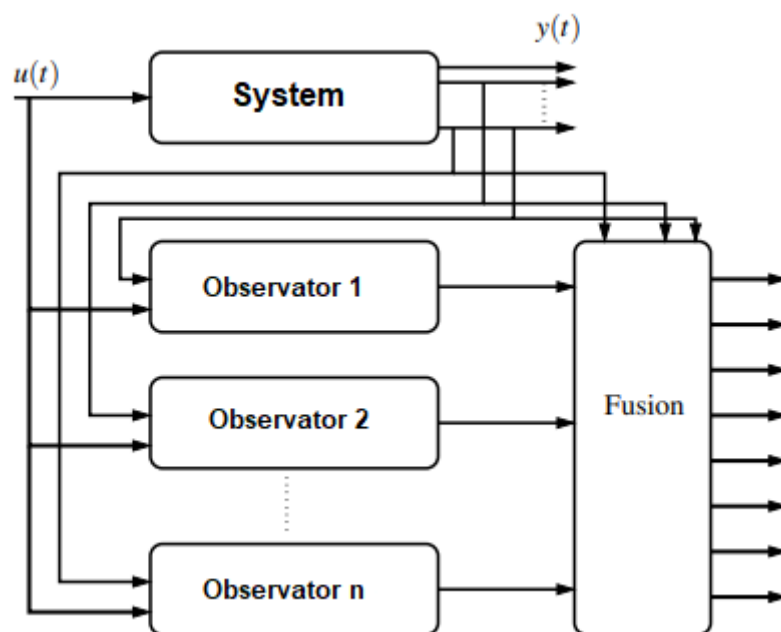

Figure 3.1: The observer's bench type DOS for sensor faults

When it is a bank of observers for sensor faults with the GOS structure, the ith observer is driven by all outputs and all inputs except the ith input.
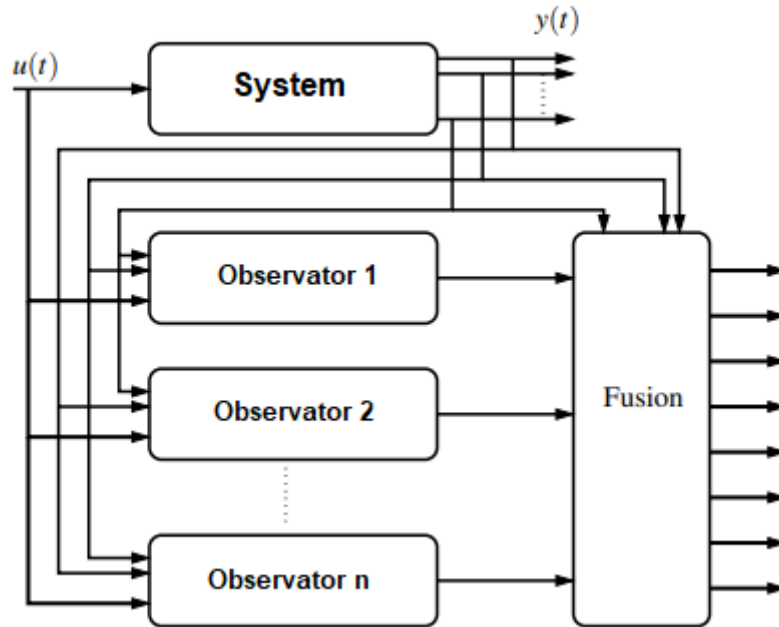

Figure 3.2: The observer's bench type GOS for sensor faults

These observers are developed to design residue generators, which are used to detect the presence of significant changes in order to provide reliable detection, and are coupled with some decision logic that constitutes a residue evaluation module with the aim of locating faults. Indeed, most of the time, the values of the residues are, at each moment, compared to thresholds. When the value of the residue is below the threshold, a Boolean value of 0 is assigned, and a Boolean value of 1 is assigned if the value of the residue has exceeded the threshold. The set of these boolean values forms a binary vector called fault signature. We then build a table that we call the theoretical signature table, such that the column j corresponds to the fault f_j and the row i corresponds to the residue r_i . The interpretation of this table allows the localization of the corresponding faults.

3.4.2   FDI bloc

This combination of residue generation and evaluation constitutes a fault detection and isolation block:
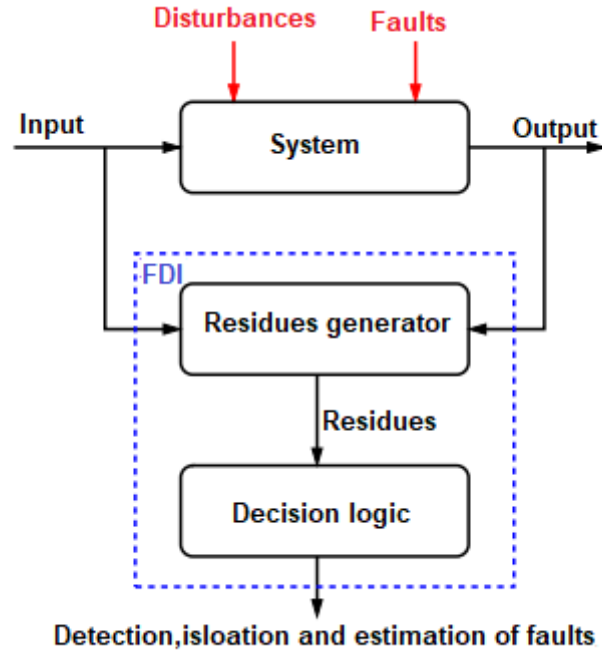
Figure 3.3: Principle of the diagnosis

3.4.3 Diagnosis by PI observer

This observer provides an estimate of the unknown input simultaneously with the state of the system, after an increase of this state, we will study the case of measurable decision variables. measurable decision variables. Consider the following T-S multi-model:

$$\begin{cases} \dot{x}(t) = \sum_{i=1}^{r} T_i(z(t)).(A_i x(t) + B_i u(t) + E_i d(t)) \\ y(t) = \sum_{i=1}^{r} T_i(z(t)).(C_i x(t) + G_i d(t)) \end{cases} \tag{3.4}$$

with : $d(t) \in R^{n_d \times 1}$ is the unknown input, and n_d is the number of defects present, in the theoretical development we assume that assumed that:

$$\dot{d} = 0 \tag{3.5}$$

E_i and G represent the distribution matrices of the unknown input on the input and the output output respectively (actuator faults and sensor faults).
In our case, we are only interested in sensor faults, therefore we take $E_i = 0$ and T-S multi-model is given then by:

$$\begin{cases} \dot{x}(t) = \sum_{i=1}^{r} T_i(z(t)).(A_i x(t) + B_i u(t)) \\ y(t) = \sum_{i=1}^{r} T_i(z(t)).(C_i x(t) + G_i d(t)) \end{cases} \tag{3.6}$$

The PI observer is of the form :

$$\begin{cases} \dot{\hat{x}}(t) = \sum_{i=1}^{r} T_i(z(t)).(A_i \hat{x}(t) + B_i u(t) + L_{P_i}(y(t) - \hat{y}(t))) \\ \dot{\hat{d}}(t) = \sum_{i=1}^{r} T_i(z(t)).L_{I_i}(y(t) - \hat{y}(t)) \\ \hat{y}(t) = \sum_{i=1}^{r} T_i(z(t)).(C_i \hat{x}(t) + G_i \hat{d}(t)) \end{cases} \tag{3.7}$$

Posing the matrices x_a, $\overline{A_i}$, $\overline{B_i}$, $\overline{C_i}$ and $\overline{L_i}$ as follows:

$$x_a = \begin{bmatrix} x(t) \\ d(t) \end{bmatrix}, \ \overline{A_i} = \begin{bmatrix} A_i & 0 \\ 0 & 0 \end{bmatrix}, \ \overline{B_i} = \begin{bmatrix} B_i \\ 0 \end{bmatrix}, \ \overline{C_i} = \begin{bmatrix} C_i & G_i \end{bmatrix}, \ \overline{L_i} = \begin{bmatrix} L_{P_i} & L_{I_i} \\ 0 & 0 \end{bmatrix}$$

From equations 3.6 and 3.7, the augmented state is obtained as follows:

$$\begin{cases} \dot{x}_a(t) = \sum_{i=1}^{r} T_i(z(t)).(\overline{A_i}x_a(t) + \overline{B_i}u(t)) \\ y(t) = \sum_{i=1}^{r} T_i(z(t)).(\overline{C_i}x_a(t)) \end{cases} \tag{3.8}$$

As well as the augmented state estimated by:

$$\begin{cases} \dot{\hat{x}}_a(t) = \sum_{i=1}^{r} T_i(z(t)).(\overline{A_i}\hat{x}_a(t) + \overline{B_i}u(t) + \overline{L_i}(y(t) - \hat{y}(t))) \\ \hat{y}(t) = \sum_{i=1}^{r} T_i(z(t)).(\overline{C_i}\hat{x}_a(t)) \end{cases} \tag{3.9}$$

In this case, the estimation error is defined by:

$$e_a(t) = x_a(t) - \hat{x}_a(t) \tag{3.10}$$

Following an approach similar to that of equation 2.55 under the constraint of observability of the augmented model, we obtain the following theorem:

Theorem 3.1: [11] The state and unknown input estimation error $e_a(t)$ converges asymptotically to zero if there exists a symmetric positive definite matrix $P > 0$, and matrices $\overline{K_i}$ such that the following conditions are met:

$$\overline{A_i}^T P + P\overline{A_i} - \overline{C_i}^T \overline{K_i}^T - \overline{K_i}\overline{C_i} < 0 \quad i = 1,..,r \tag{3.11}$$

The observer's gains are obtained from equation :

$$\overline{L_i} = P^{-1}\overline{K_i} \tag{3.12}$$

We can also relax the conditions by the addition of matrices Q_i or a term to ensure exponential stability with a rate of convergence α (decay rate), the LMI are written as follows:

$$\overline{A_i}^T P + P\overline{A_i} - \overline{C_i}^T \overline{K_i}^T - \overline{K_i}\overline{C_i} + 2\alpha P < 0 \quad i = 1,..,r \tag{3.13}$$

We note that the previous development is made under the assumption: $\dot{d} = 0$, which theoretically means that the unknown inputs are constant, which restricts the set of signals that the PI observer manages to estimate them, nevertheless, it is practically possible to estimate low-frequency signals with slow dynamics, this implies an increase in gains, which leads to an increase in the sensitivity to measurement noise, so a trade-off must be found between robustness and performance. However, an interesting approach is used to increase the bandwidth of the observer and expand the set of signals to estimate to more dynamic signals, The idea is to generalize the design of PI observers and to use several integral actions to build the PMI (Proportional Multi-Integral) observer which simultaneously estimates the first q derivatives of the unknown input supposed to have the qth zero derivative $d^{(q)}(t) = 0$, while in the case of a PI observer, we have the first derivative of d(t) which is zero.

The applications we have made in this manuscript are limited to the case of the PI of the PI observer with measurable decision variables.

3.5 Fault tolerant control

3.5.1 FTC bloc

The FTC block is in charge of determining or resetting the control law in such a way that it is fault-tolerant. It is based on the results transmitted by the FDI block in order to keep the stability and the initial performance required by the control objectives within the desired standards. In the following we will present as an example some methods and strategies of fault tolerant control, we distinguish the methods designed for linear systems and those dedicated to linear systems and those dedicated to non-linear systems.
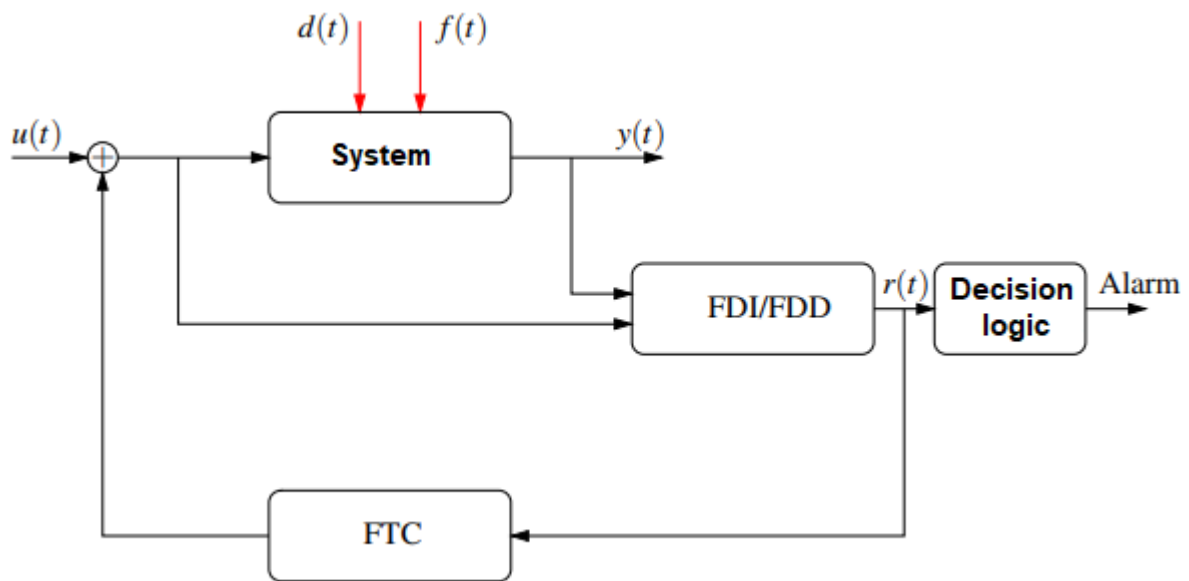

Figure 3.4: FTC Architecture

3.5.1.1 Methods for linear systems

1. Pseudo-inverse method: it is used for linear systems, the idea on which it is based is the minimization of a Frobenius norm $\|\|\|_F$ between the closed-loop model of the faulty system and the reference one. reference, consider the following linear system :

$$\begin{cases} \dot{x}(t) = Ax(t) + Bu(t) \\ y(t) = Cx(t) \end{cases}$$

This equation describes the dynamics of the system in the nominal case, in order to stabilize it or to obtain specific performances we consider that the system is controlled by state feedback $u(t) = Kx(t)$ under controllability constraints. In closed loop we have :

$$\begin{cases} \dot{x}(t) = (A + BK)x(t) \\ y(t) = Cx(t) \end{cases}$$

Now, when a fault has occurred, the modification caused by the fault leads to the following model :

$$\begin{cases} \dot{x}_f(t) = A_f x_f(t) + B_f u_f(t) \\ y_f(t) = C_f x_f(t) \end{cases} \tag{3.14}$$

The index f indicates a faulty situation, the pseudo-inverse method consists in determining the control law $u_f(t) = K_f x_f(t)$ for the faulty system, in such a way that its dynamics is as close as possible to the sane system , which leads to :

$$A + BK = A_f + B_f K_f \tag{3.15}$$

We then want to minimize the criterion J given by the following Frobenius norm:

$$J = \|(A + BK) - (A_f + B_f K_f)\| \tag{3.16}$$

The minimization of the error in the least squares sense gives :

$$K_f = B_f^+ (A + BK - A_f) \tag{3.17}$$

with B_f^+ is the pseudo-inverse of the matrix B_f.
The great advantage of this method is its simplicity and ease of implementation, however, it has the disadvantage of not guaranteeing stability in closed loop, constraints have been imposed in this context but this increases considerably the computation time, another disadvantage lies in the fact that it requires a perfect knowledge of the faulty model (the matrices A_f, B_f and C_f), which may lead to modeling uncertainties, the extension of this method to the nonlinear case also represents a limitation.

2. Method by placing own structure: this method aims at making coincide the eigenvalues of the matrices of the system without faults in closed loop (the matrix $A + BK$) with those of the faulty system (the matrix $A_f + B_f K_f$), and this by minimizing the norm 2 $\|\|_2$ between the various corresponding eigenvectors, the objective being to find the gain K_f which manages to check this, Indeed, the eigenstructure (eigenvalues and eigenvectors) determine the temporal response of the system, so the goal is to impose a dynamic to the faulty system as close as possible to that of the nominal system, it is a form of pole placement so that they coincide with each other. Contrary to the pseudo-inverse method, this one does not pose much of a problem as far as the guarantee of the stability in closed loop or the computational load is concerned, however it also has the disadvantage of the difficulty of taking into account the modeling uncertainties, since it supposes the possession and the knowledge of the matrices A_f , B_f and C_f.

3.5.1.2   Methods for non linear systems

There are several approaches to FTC control, in the following we cite a few as examples.
1. Method based on controller bench: it is based on the existence of a bank of pre-calculated controllers, each one is dedicated to a certain mode of operation, several scenarios are considered, for each one a model is implemented and a controller is synthesized, algorithms are thus conceived for the switching between the laws of control according to a certain logic, the main idea consists in determining the previously synthesized controller which corresponds best to the faulty situation, This is done by a supervisor made up of

estimators that uses the information provided by them (FDI block) to select the closest one to the system after comparing the estimated values with the measured values, the estimator with the minimum error is chosen, the corresponding controller is applied to elaborate the control law, however, it has limitations when unlisted faults appear or when the number of models increases with the increase of the faults considered simultaneously.

2. Fuzzy logic based method: it deals with non-linear systems and includes multi-models, the accommodation technique is based on an adaptive fuzzy control allowing the on-line learning of new unknown dynamics caused by the appearance of faults, this active approach consists in using fuzzy models of Takagi-Sugeno type as well as observers and observers and fuzzy controllers.

3.5.1.3 Fault tolerant control by trajectory tracking

There is another interesting approach that uses a reference model, it is used mainly for tracking, the states and faults estimated by the FDI block are used by the FTC block to add a new term in the control law, in fact, if no fault has been detected the term added is almost zero, otherwise, the estimation of the magnitude of this fault and its subtraction from the measurement or the real magnitude leads to add a term in the control law thus allowing the compensation of the fault.
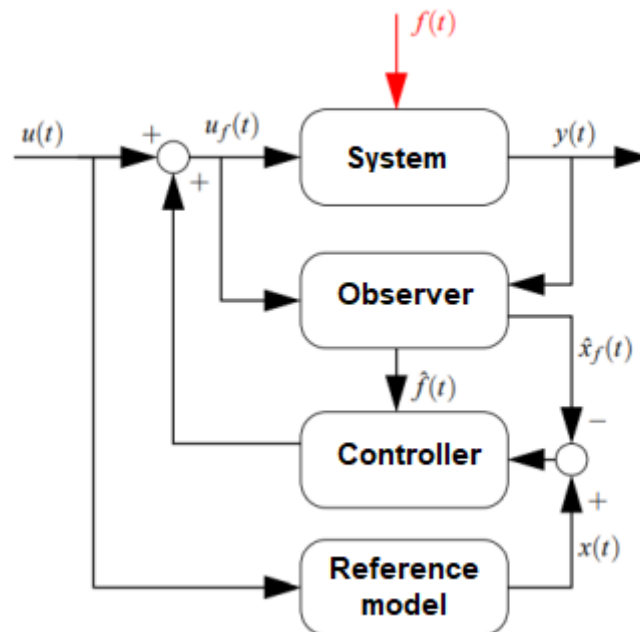

Figure 3.5: FTC based on a reference model

The strategy adopted for the application on multi-models is based on the use of a PI (or PMI) observer, in order to estimate the faults, then they will be taken into account for the synthesis of the control law as explained previously. If we consider that the fuzzy multi-model in the presence of sensor faults only is modeled by the following representation:

$$\begin{cases} \dot{x}_f(t) = \sum_{i=1}^{r} T_i(z(t)).(A_i x_f(t) + B_i u_f(t)t) \\ y(t) = \sum_{i=1}^{r} T_i(z(t)).(C_i x_f(t) + G_i d(t)) \end{cases} \tag{3.18}$$

the control law is given by :

$$u_f(t) = \sum_{i=1}^{r} T_i(z(t)).(u(t) + K_i(x(t) - \hat{x}_f(t))) \tag{3.19}$$

K_i matrices are determined to ensure system stability and minimize deviation between $x_f(t)$ and $x(t)$.

The analysis of the control law proposed in (3.19) requires the knowledge of the vector of faults f(t) through its estimation. This estimation is obtained via a PI observer which simultaneously estimates the state of the faulty system and the fault vector.

u(t) is the control signal allowing to realize the trajectory tracking without the presence of faults.

3.6 Conclusion

This chapter has been devoted to present the different concepts and tools needed for the development of a fault tolerant control, whose approaches are classified into passive and active approaches, the major interest has been given to the latter approach, the former is just a robust control without any online intervention. The principle and structure of the active approach and some of its methods were presented. We also introduced the notion of system observation and its application for T-S fuzzy models, in particular, the PI observer which was used for the simultaneous estimation of the state and the faults, this estimation was used directly by the FTC block for the fault compensation and the elaboration of the new control law, the effects of the different factors affecting the system have been showed, the adopted strategy gives good results for slowly varying faults. The limitations of the approach are also presented when the dynamics of the references or the faults are faster. In all cases a compromise between speed and stability must be ensured (performance versus robustness).

Chapter 4

Application to the regulation of the inter-distance between two vehicles

4.1   Introduction

In this section, we present the results of the simulation that we have done by presenting some possible scenarios. First, we start by simulating the model in free regime without the leading vehicle. Then, a simulation is performed in closed loop with a stabilizing control with and without LMI relaxation, an observer to estimate the states is also synthesized. Then, a simulation is performed in the presence of the leading vehicle to regulate the vehicle inter-distance. Finally, a control law for the stabilization is developed using fault tolerant control and diagnostic techniques.

Notes:

The resolution of the LMI is always done by Matlab, and based on the "LMI Control Toolbox".

The theorems presented in chapter 2 ensure global convergence, i.e. the choice of the initial conditions does not influence the stability.

The linear TS models weighted by normalized activation functions allow to represent without approximation the global nonlinear system. Therefore, the representation of the system by its nonlinear model or by its TS model give exactly the same results.

4.2   Simulation in free regime

We apply the theorem (2.1) in order to study the stability of the electric vehicle model given by (2.11).

We find that there exists a matrix P that is symmetric and positive define, $P = \begin{bmatrix} 1.043 & 0.001 \\ 0.001 & 0.0255 \end{bmatrix}$, we can also check the define positivity by finding its eigenvalues: $eig(P) = \{0.0255, 1.043\}$ that all are positive. We conclude that the system is stable.

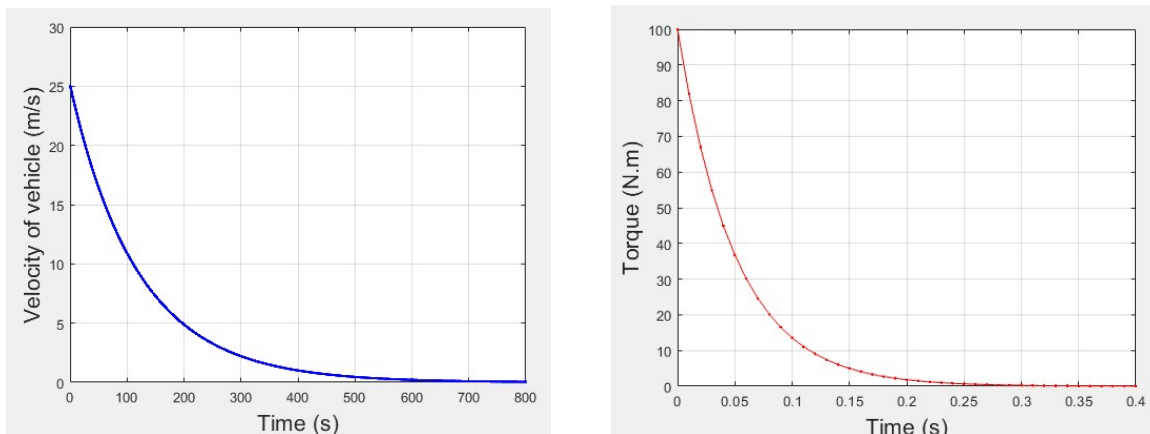We take as initial state: $x_0 = \begin{bmatrix} 25 \\ 100 \end{bmatrix}$

Figure 4.1: System states in open-loop

Commentaries and conclusion

We see that all the states of the system converge towards the origin, i.e. $x(t) = 0$, and the response time is 700s.

We conclude that in the case of absence of head vehicle, i.e. open-loop, the system is stable. However, the response time is very large (due to the forces of friction with the road that are not taken into account). Hence, the synthesis of stabilizing control laws to improve performance are required.

4.3   Closed loop simulation

4.3.1   Stabilization of EV based on TS fuzzy model

In this part, we consider a PDC control to stabilize the system and ensure the braking of the vehicle.

4.3.1.1   PDC Without LMI relaxation

We apply the theorems (2.25) and (2.26) in order to find a PDC control that stabilize the system, its model is given by equation (2.11).

The state feedback command law is given by equation (2.18), and the K_i parameters are calculated by equation (2.27).
We find : $K_1 = \begin{bmatrix} 0.0132 & -0.9738 \end{bmatrix}$ and $K_2 = \begin{bmatrix} 0.0131 & -0.9738 \end{bmatrix}$
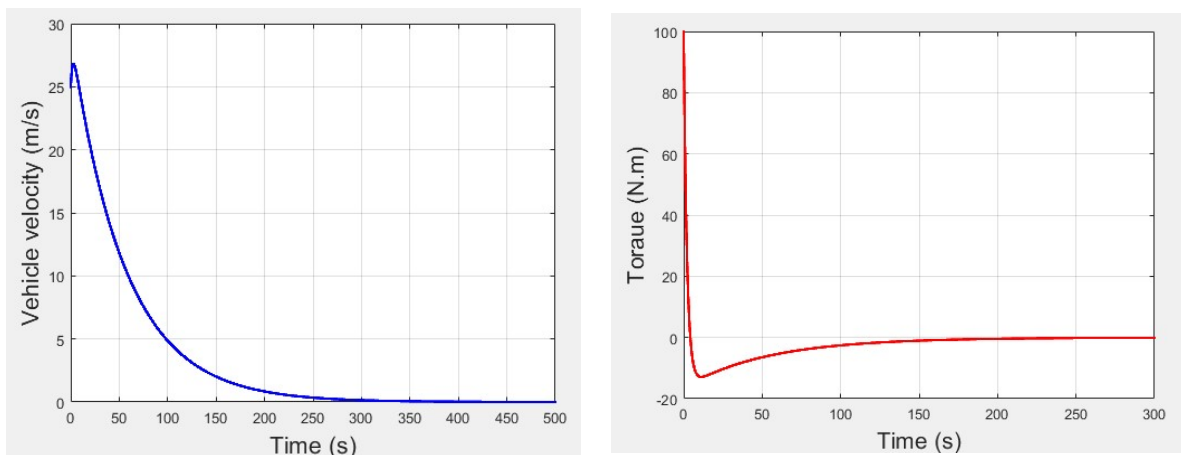We take as initial state : $x_0 = \begin{bmatrix} 25 \\ 100 \end{bmatrix}$
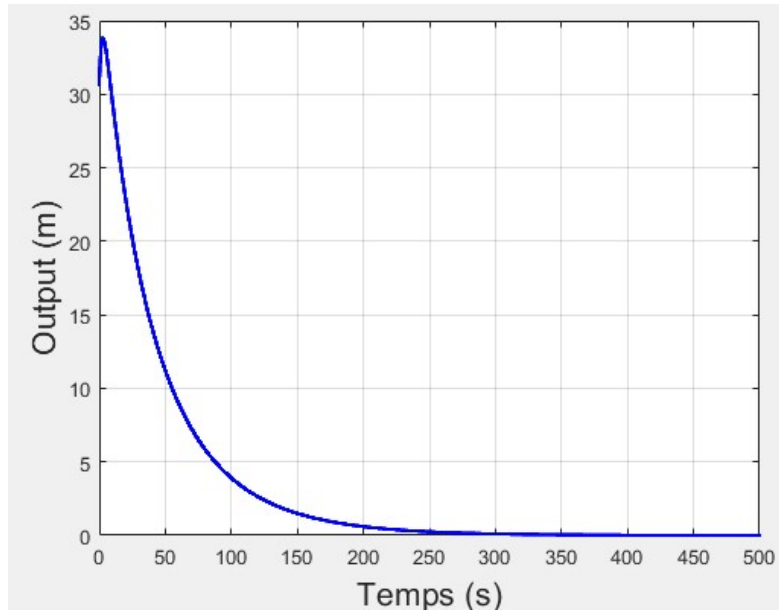

Figure 4.2: System states with PDC

Figure 4.3: System output with PDC

Commentaries and conclusion

We see that all the states of the system converge towards the origin, i.e. $x(t) = 0$, same as the output which is the difference between the set point of the safety distance and the minimum safety distance $(y(t) = d(t) - d_{min})$ converges to 0 which means that the stationary safety distance must be equal to the minimum safety distance. We also observe that the response time is $300s$ which is relatively small compared to the previous simulation.

We conclude that PDC method is used to ensure the stability of the looped multi-models and to improve and speed up the dynamics of the system. However, solving the LMIs gives a random matrix P (that still satisfies the conditions of stablization), but we do not choose the poles or the dynamics of the system, as a consequence the method of pole placement is needed to improve the system's performance further.

4.3.1.2 PDC With LMI relaxation

We apply the theorems (2.30) and (2.31) in order to find a PDC control with LMI relaxation that stabilizes the system, its model is given by equation (2.11).
The state feedback command law is given by equation (2.18), and the K_i parameters are calculated by equation (2.27).
We find : $K_1 = \begin{bmatrix} 111.644 & -46.7938 \end{bmatrix}$ and $K_2 = \begin{bmatrix} 111.8570 & 46.9284 \end{bmatrix}$

We take as initial state : $x_0 = \begin{bmatrix} 25 \\ 100 \end{bmatrix}$
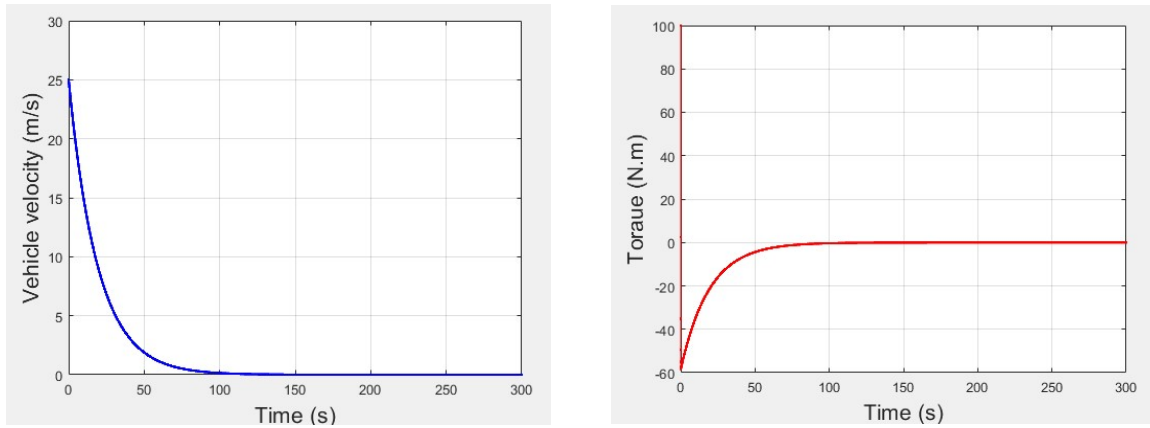
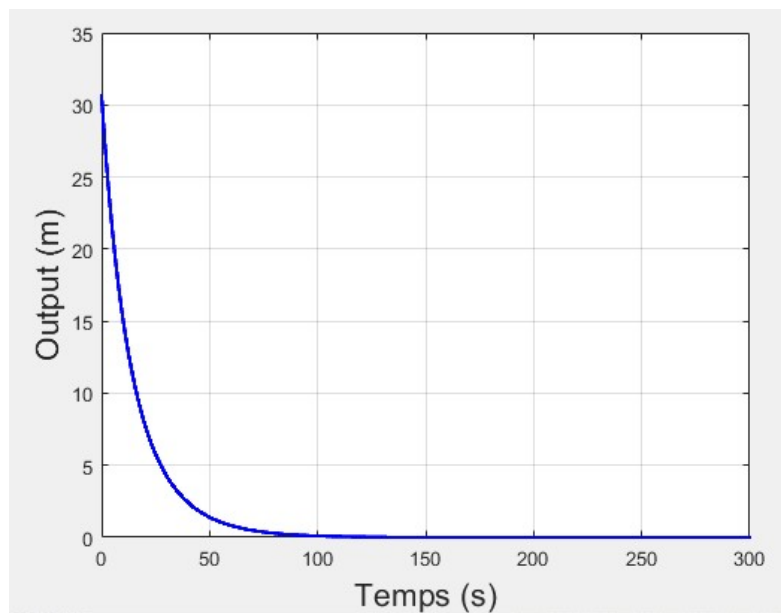Figure 4.4: System states with PDC+LMI relaxation

Figure 4.5: System output with PDC+LMI relaxation

Commentaries and conclusion

We see that all the states of the system converge towards the origin, i.e. $x(t) = 0$, same as the output. We also observe that the response time is reduced to $100s$ which is even smaller compared to the previous simulations.

We conclude that LMI relaxation is used to solve the major disadvantage of using the Lyapunov function that lies in obtaining very conservative stability conditions, which can be relieved.

4.3.2   Estimation of Electric vehicle's states

4.3.2.1   State estimation Without LMI relaxation

The resolution of the LMI system presented by the inequalities (3.23) gives the fol-

lowing gains:

$$L_1 = \begin{bmatrix} 0.1175 \\ 0.1060 \end{bmatrix} \qquad L_2 = \begin{bmatrix} 0.2601 \\ 0.1361 \end{bmatrix}$$

We take as initial state : $x_0 = \begin{bmatrix} 25 \\ 100 \end{bmatrix}$

and for the estimated initial state : $\hat{x}_0 = \begin{bmatrix} 15 \\ 70 \end{bmatrix}$
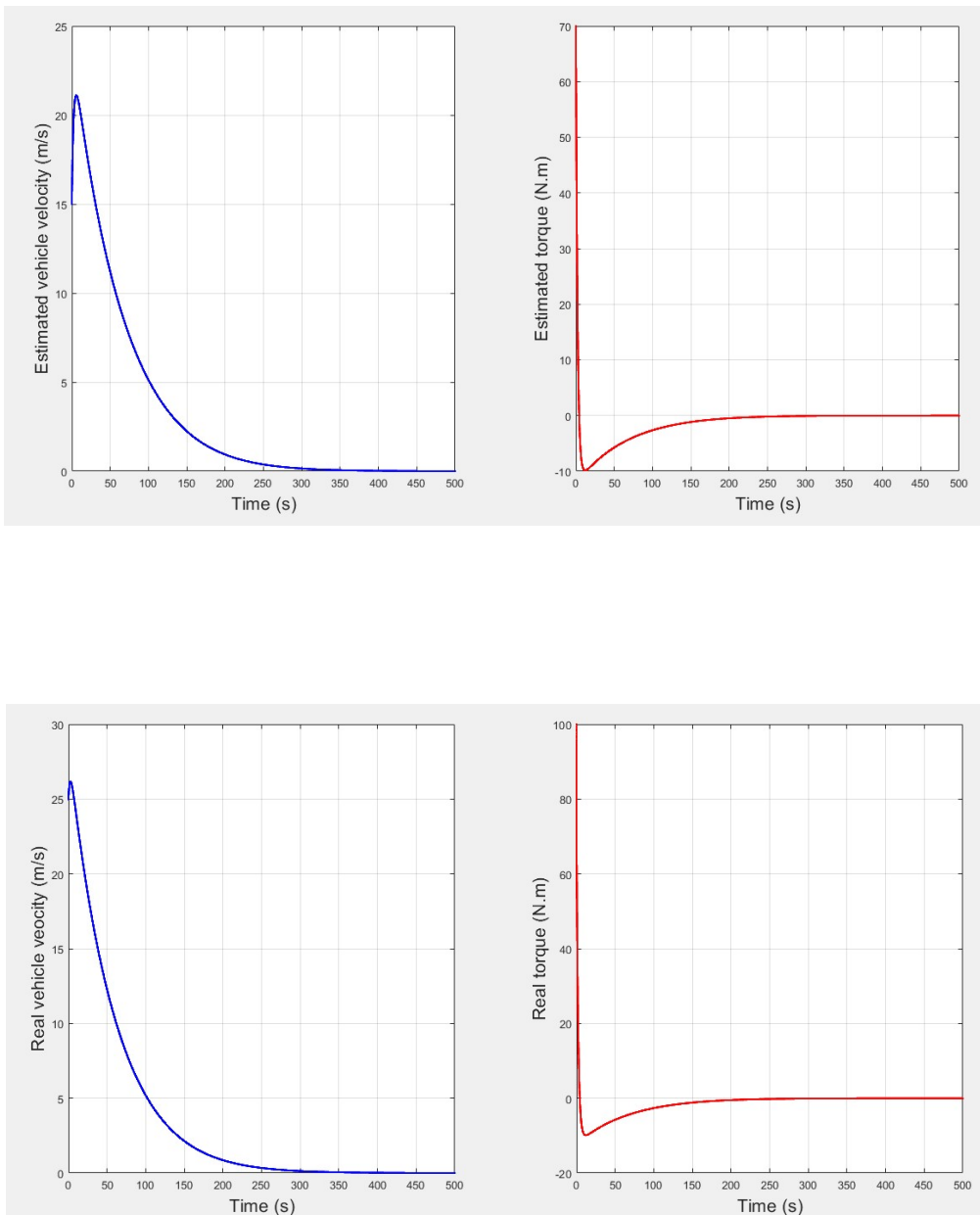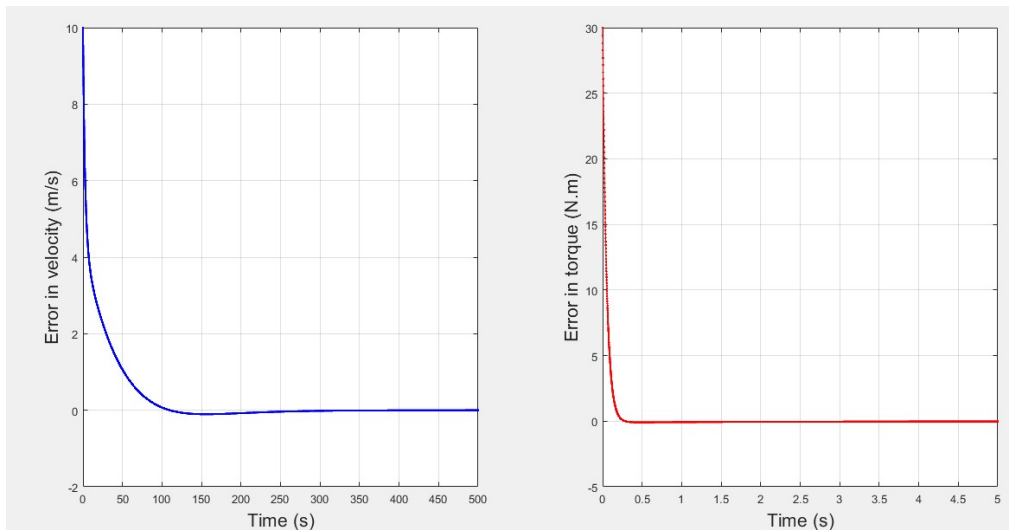

Figure 4.6: System states with observer

Figure 4.7: System output with observer

Commentaries and conclusion

We see that all the estimated states of the system are similar to the real states despite the difference in initial conditions. We also observe that the error between the real and estimated states converge towards 0 in $100s$ which is more quicker than the output (converges in $300s$ 4.13.

We conclude that an observer is needed to estimate the states of the system that will be used in the synthesis of the PDC control law .Hence, the dynamics of the observer must be faster than the state feedback controller's dynamics and that is required to compensate the estimation error on the controller performance.

4.3.2.2   State estimation With LMI relaxation

The resolution of the LMI system presented by the inequalities (3.23) gives the following gains:

$$L_1 = \begin{bmatrix} 0.1175 \\ 0.1060 \end{bmatrix} \qquad L_2 = \begin{bmatrix} 0.2601 \\ 0.1361 \end{bmatrix}$$

We take as initial state : $x_0 = \begin{bmatrix} 25 \\ 100 \end{bmatrix}$

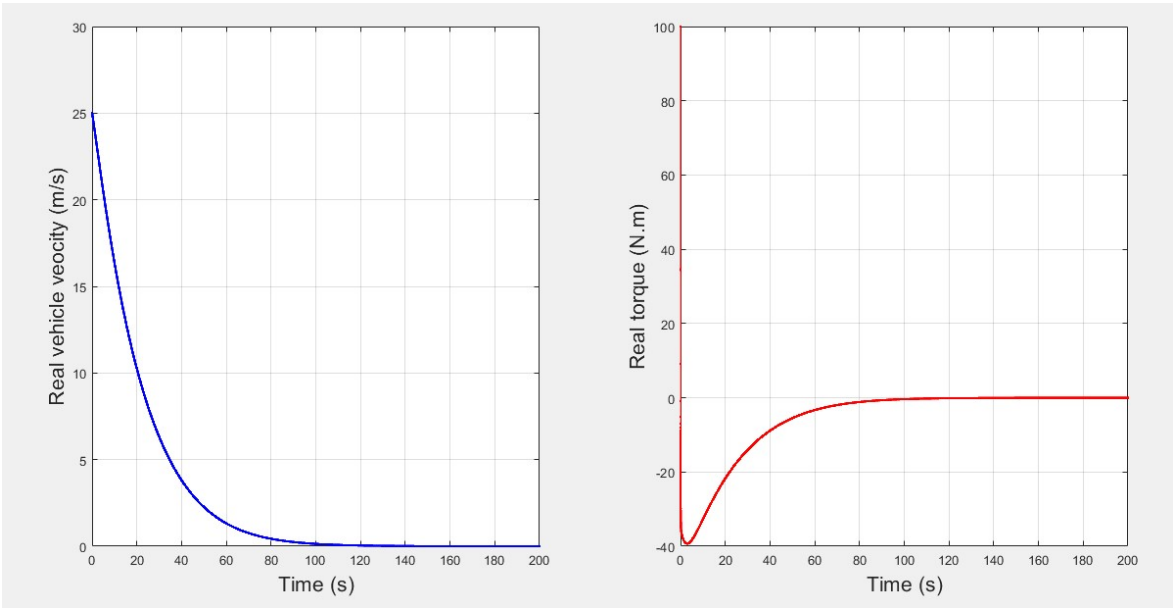and for the estimated initial state : $\hat{x}_0 = \begin{bmatrix} 15 \\ 70 \end{bmatrix}$
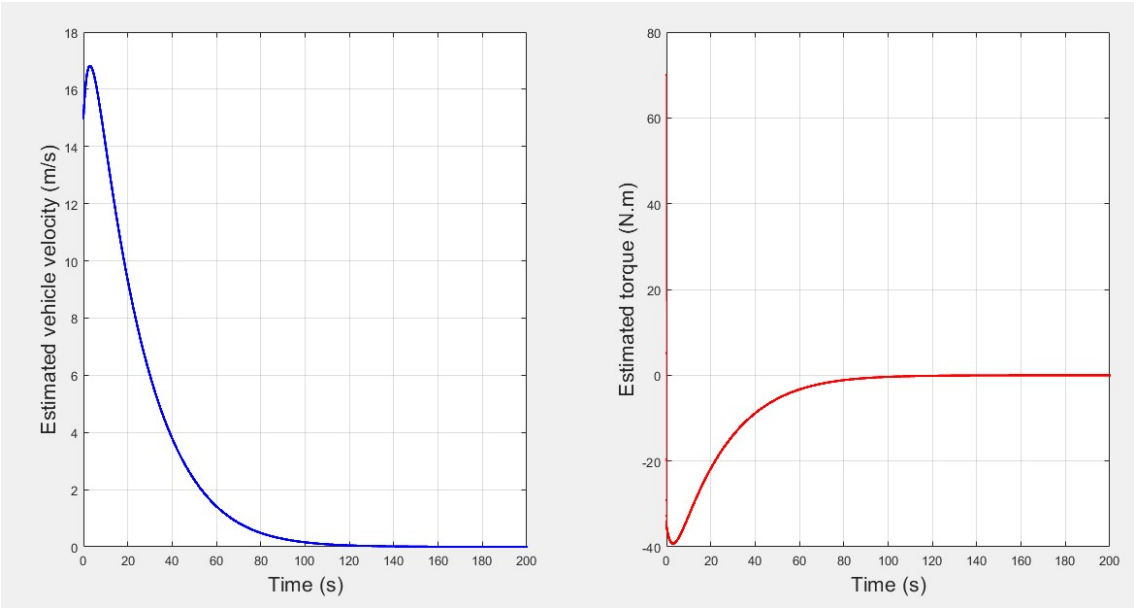
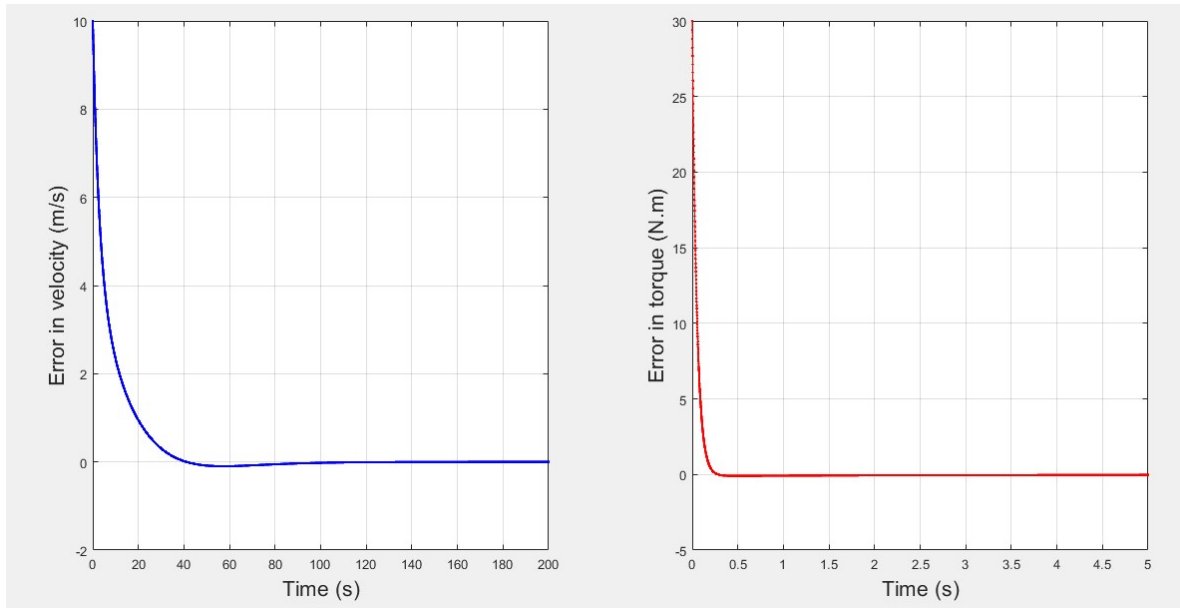Figure 4.8: System states with observer

Figure 4.9: System output with observer

Commentaries and conclusion

We see that all L_i gains of the observer are the same with and without the usage of LMI relaxation. We also observe that the error between the real and estimated states converge towards 0 in $40s$ which is more quicker than the output (converges in $100s$ 4.5.

4.3.3 Trajectory tracking with integral structure

The Takagi-Sugeno model of the electric vehicle is given by the equation 2.12.
We compute the augmented model:

$$
\begin{cases}
\overline{A_1} = \begin{bmatrix} -\frac{a_x + b_x.v_{max}}{\alpha} & \frac{R_{ap}}{\alpha} & 0 \\ 0 & -\frac{1}{\tau_e} & 0 \\ -e - f.v_{max} & 0 & 0 \end{bmatrix}, \overline{B_1} = \begin{bmatrix} 0 \\ \frac{1}{\tau_e} \\ 0 \end{bmatrix}, \\
\overline{A_2} = \begin{bmatrix} -\frac{a_x + b_x.v_{min}}{\alpha} & \frac{R_{ap}}{\alpha} & 0 \\ 0 & -\frac{1}{\tau_e} & 0 \\ -e - f.v_{min} & 0 & 0 \end{bmatrix}, \overline{B_2} = \begin{bmatrix} 0 \\ \frac{1}{\tau_e} \\ 0 \end{bmatrix},
\end{cases}
$$

The resolution of the LMI system presented by the inequalities (3.33) and (3.34) gives the following gains :

$$K_1 = \begin{bmatrix} 0.8116 & -0.9264 \end{bmatrix} ; K_2 = \begin{bmatrix} 0.9912 & -0.9114 \end{bmatrix}$$
$$M_1 = -0.054 ; M_2 = -0.071$$

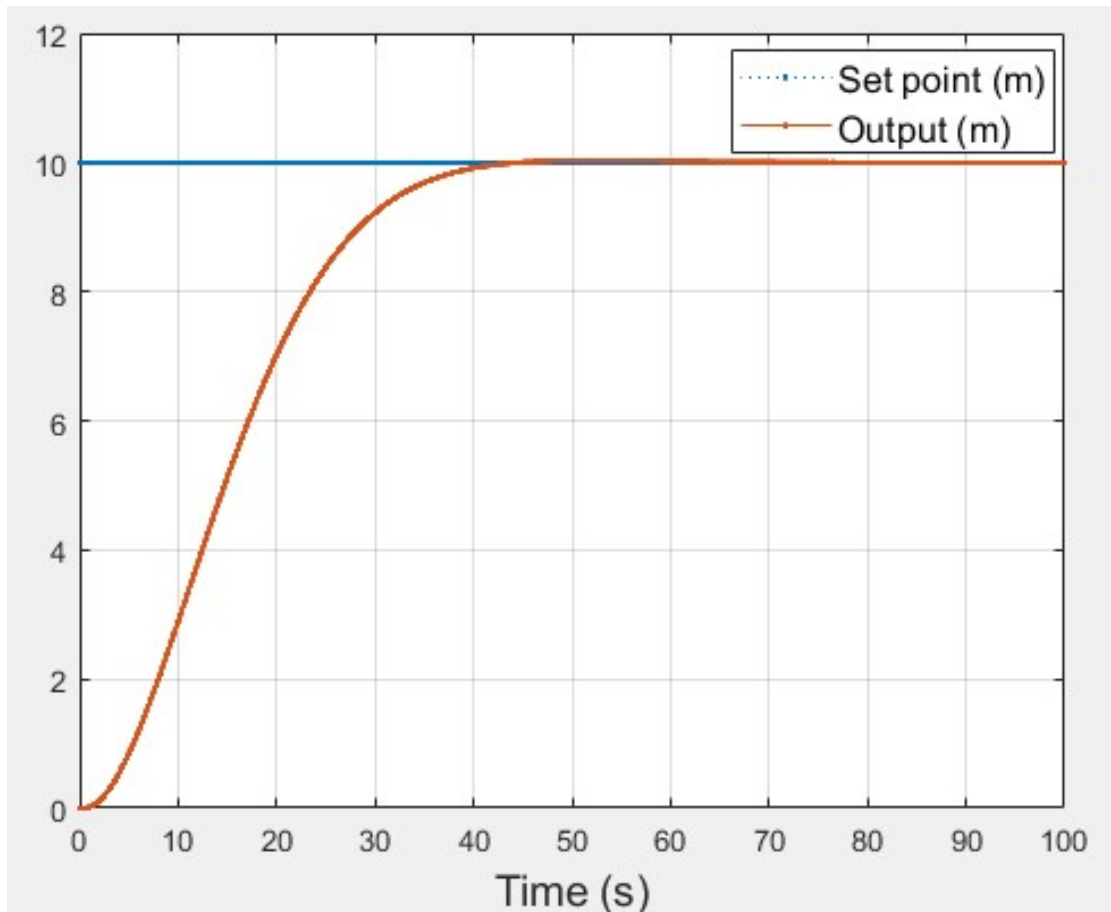We take as initial state : $x_0 = \begin{bmatrix} 0 \\ 0 \end{bmatrix}$

Figure 4.10: The step response of the system

Commentaries and conclusion

We notice that the nonlinear system is well stabilized by the PDC type control law and thus the tracking of the set point is well ensured. On the other hand, the performance of the system remains poor (the response time of the system is high (28.5s) and the oscillations are not desirable) and requires the improvement of the set of LMI conditions that we found.

4.3.4 Performance improvement by pole placement

The Takagi-Sugeno model of the electric vehicle is given by the equation 2.12.

4.3.4.1 Stabilization case

The resolution of the LMI system presented by the inequalities (2.92),(2.93) and (2.94) gives the following gains :

$$K_1 = \begin{bmatrix} 2847.73 & 69.02 \end{bmatrix} \; ; \; K_2 = \begin{bmatrix} 3611.6 & 96.66 \end{bmatrix}$$

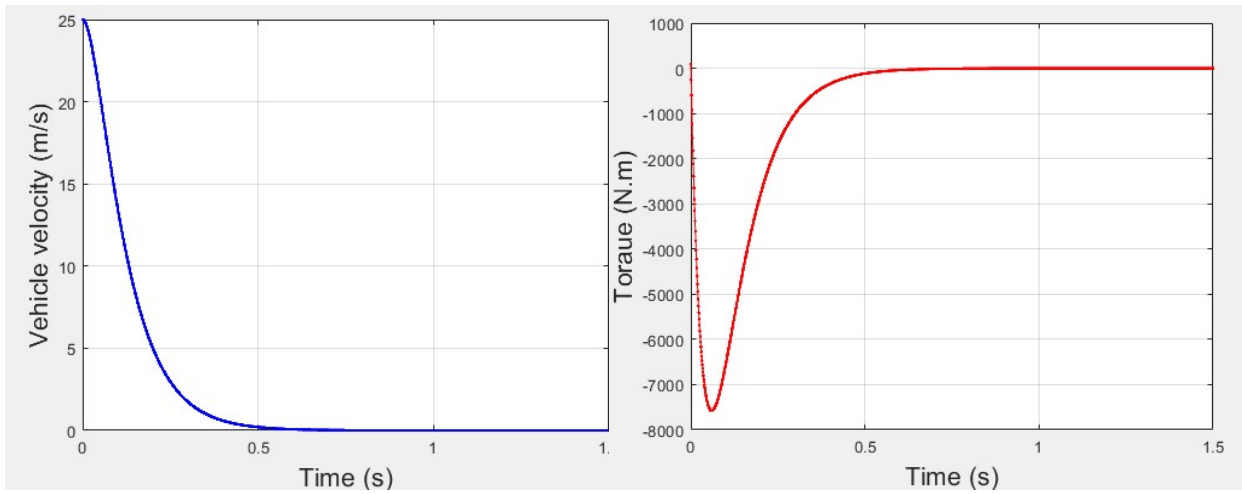We take as initial state : $x_0 = \begin{bmatrix} 0 \\ 0 \end{bmatrix}$
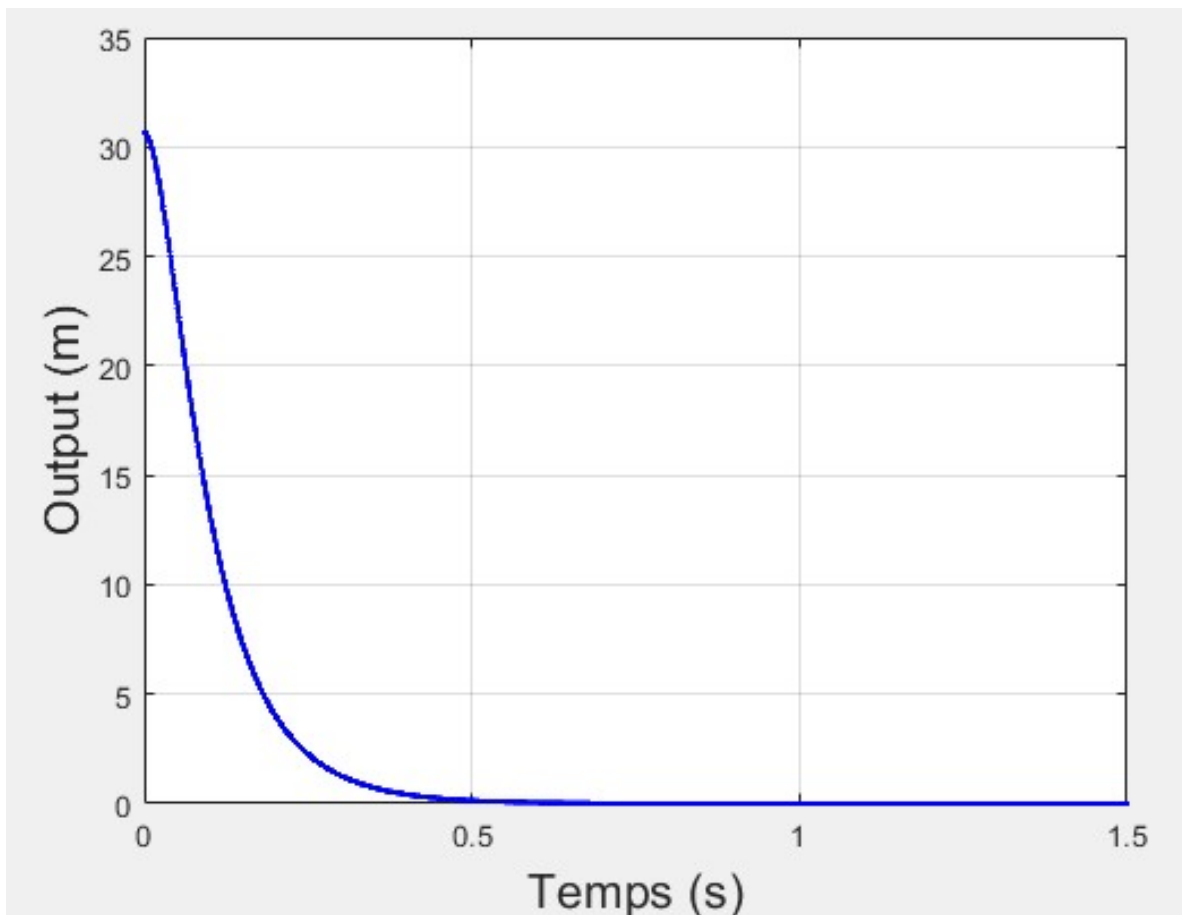

Figure 4.11: System states with PDC + PP

Figure 4.12: System output with PDC + PP

4.3.4.2 Trajectory tracking case

The resolution of the LMI system presented by the inequalities (2.92),(2.93) and (2.94) gives the following gains :

$$K_1 = \begin{bmatrix} 4984.3 & 287.02 \end{bmatrix} \; ; \; K_2 = \begin{bmatrix} 5130.6 & 298.6 \end{bmatrix}$$
$$M_1 = -8171.8 \; ; \; M_2 = -8468.1$$

We take as initial state : $x_0 = \begin{bmatrix} 0 \\ 0 \end{bmatrix}$
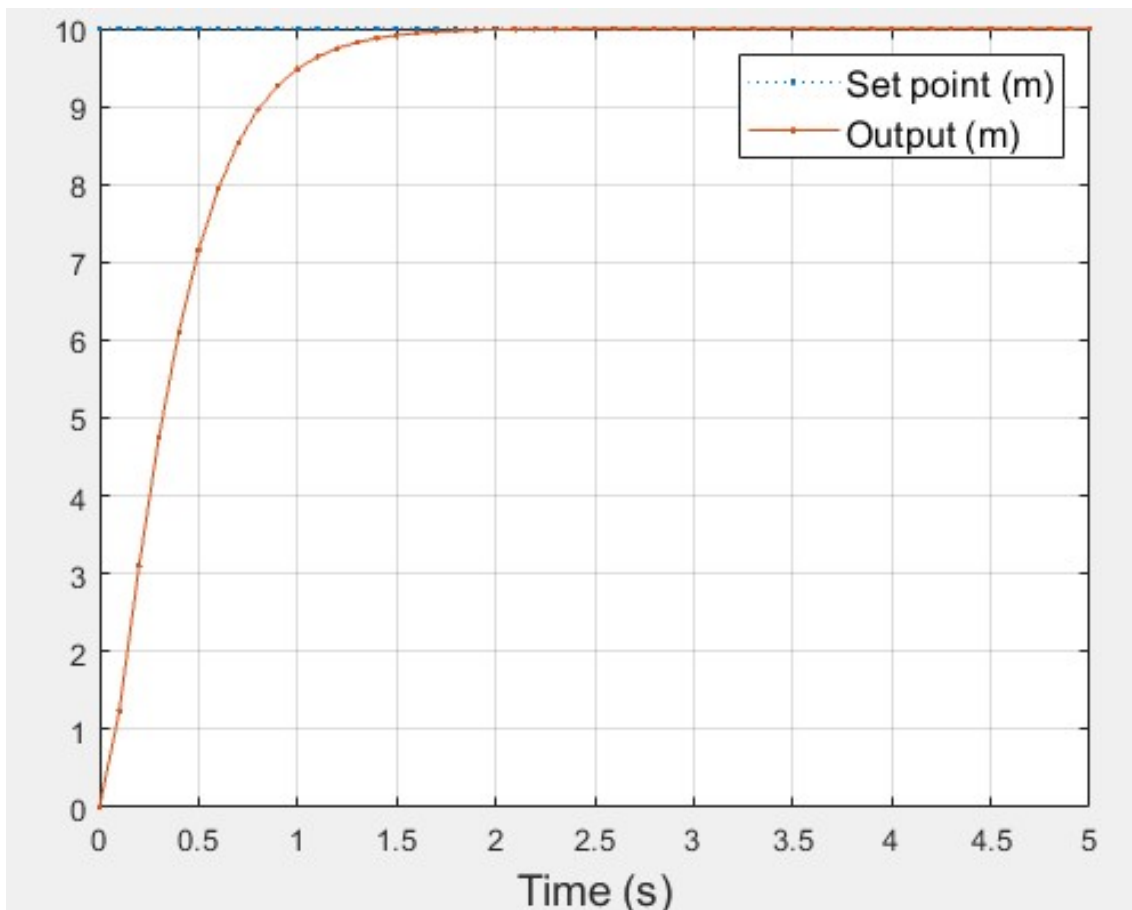

Figure 4.13: The step response of the system

Commentaries and conclusion

We see in figure (4.11) and (4.12) that all the states of the system converge towards the origin, i.e. $x(t) = 0$, same as the output. We also observe that the response time is reduced to 0.5s which is much smaller compared to the simulations that are done without pole placement. We also see in figure (4.13) that the output of the system is able to pursue the set point without overshoot and without oscillations, and the response time is 1.5s which is inferior than 40s in the case of trajectory tracking with integral structure only. We notice that the method by placing poles gives better performances. Indeed, the dynamics of the system presented in figures (4.12) and (4.13) is very well improved compared to the case without pole placement presented in figures (4.3) and (4.10) .

4.4 Simulation of trajectory tracking

In this part, the simulations have been performed taking into account the leading vehicle. In practice, the distance between the two vehicles is provided by a sensor. The objective of the control is to ensure the convergence of the distance inter-vehicle distance (Δx) to the safety distance $d(t)$.

By analyzing the distance error $(e = \Delta x - d(t))$, we distinguish two cases:

Positive error case : the inter-vehicular distance is greater than the safety distance imposed by the model. This error, even if it is large does not have a negative impact on the safety of the vehicle.

Negative error case : the inter-vehicular distance is less than the safety distance imposed by the model. In practice, it must be minimal compared to a predefined threshold on condition that the error in absolute value remains lower than the minimal safety distance.
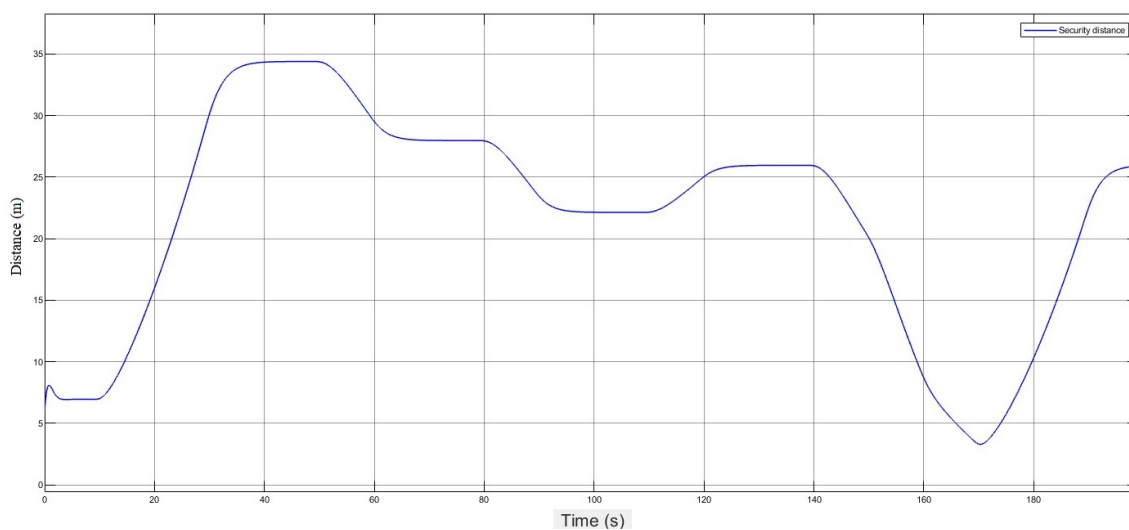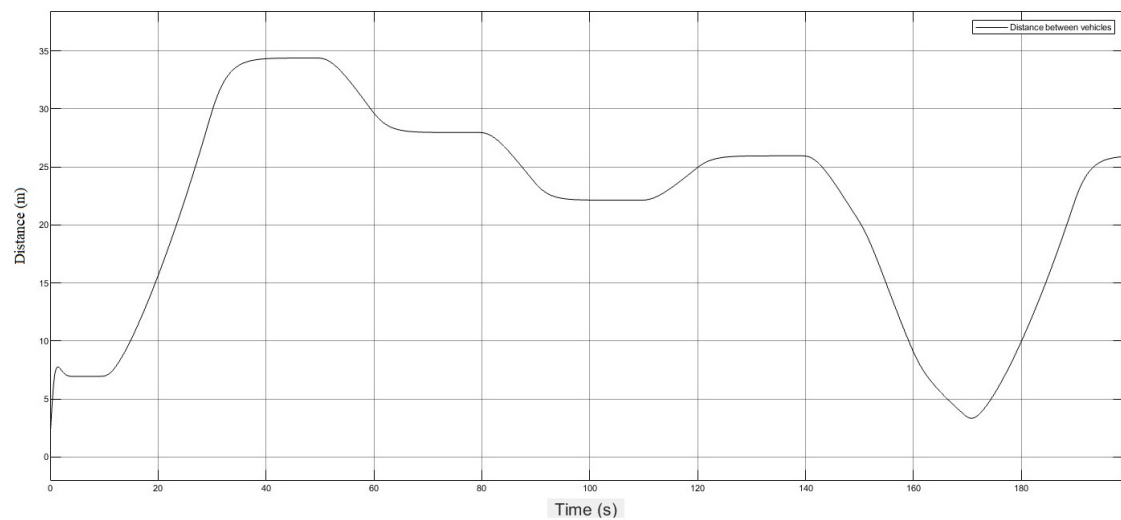

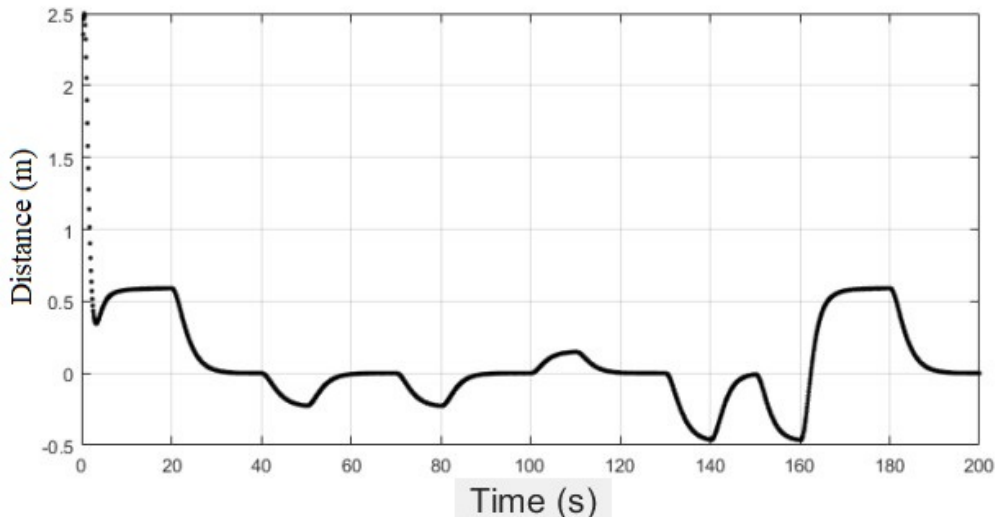Figure 4.14: Tracking of the safety distance set point
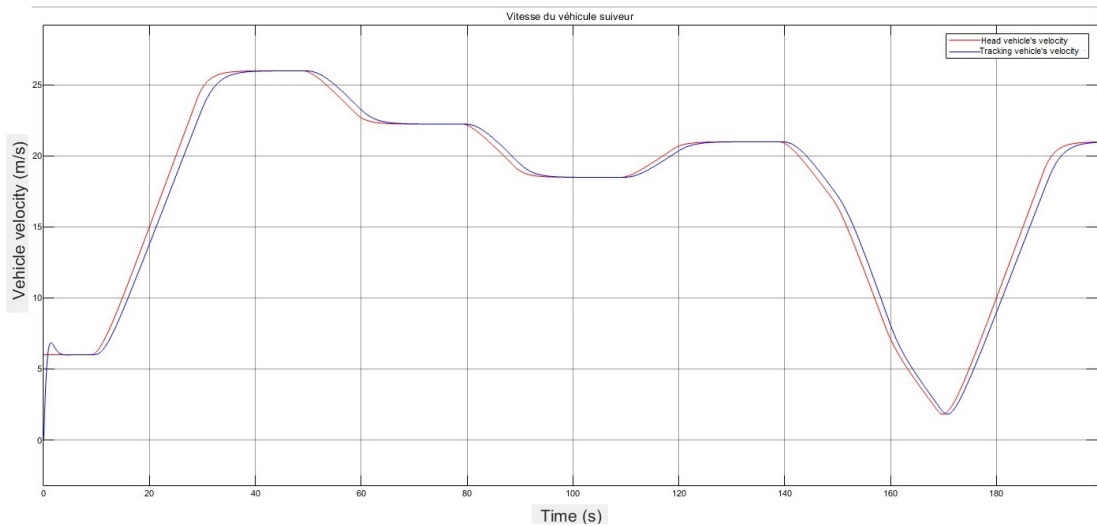
Figure 4.15: Error of the safety distance

Figure 4.16: The vehicle velocity profile

Commentaries and conclusion

We notice that the inter-vehicular distance converges to the safety distance with a response time of 0.5s.

By analyzing the velocity profile, we notice that the velocity of the following vehicle takes time to catch up with the velocity of the leading vehicle, this is normal due to the dynamics of the two vehicles which are not the same. We can take the example of a standard vehicle and a sports vehicle   The main objective of this simulation is to leave a safe inter-vehicle distance in order to allow the driver to operate his vehicle safely and avoid the collision. In order to verify the effectiveness of the control law, an emergency braking situation of the leading vehicle was performed.

It can be seen that the following distance given by figure (4.14) is always respected with respect to the set point. By Therefore, both vehicles stop without colliding.

4.5   Sensor fault tolerant control

It is assumed that a fault d(t) is injected into the system, this fault affects the sensors. The resolution of the LMI system presented by the inequalities (3.13) gives the following gains:

$$K_1 = \begin{bmatrix} 24.7472 & 0.9055 \end{bmatrix} \; ; \; K_2 = \begin{bmatrix} 5.7185 & 0.7939 \end{bmatrix}$$

$$\overline{L_1} = \begin{bmatrix} 338.9506 \\ 67.7447 \\ 136.1944 \end{bmatrix} \; ; \; \overline{L_2} = \begin{bmatrix} -539.2826 \\ -112.4616 \\ -216.7539 \end{bmatrix}$$

The results of the simulations are shown on the following cases depending on the frequency of the fault:

4.5.1   Simulation of results for biased faults

Biased faults are constant signals, they are special case of sinusoidal signals and are obtained with a zero frequency.

Figure 4.17: Sensor fault estimation with a PI observer

Figure 4.18: Correction of the output in the presence of faults

Figure 4.19: Error between the output of good sensor and corrected output

4.5.2 Simulation of results for faults slowly varying

In order to simulate a slowly varying fault, we inject a sinusoidal signal with a small frequency.

Figure 4.20: Sensor fault estimation with a PI observer

Figure 4.21: Correction of the output in the presence of faults

Figure 4.22: Error between the output of good sensor and corrected output

4.5.3 Simulation of results for faults quickly varying

In order to simulate a quickly varying fault, we inject a sinusoidal signal with a bigger frequency.
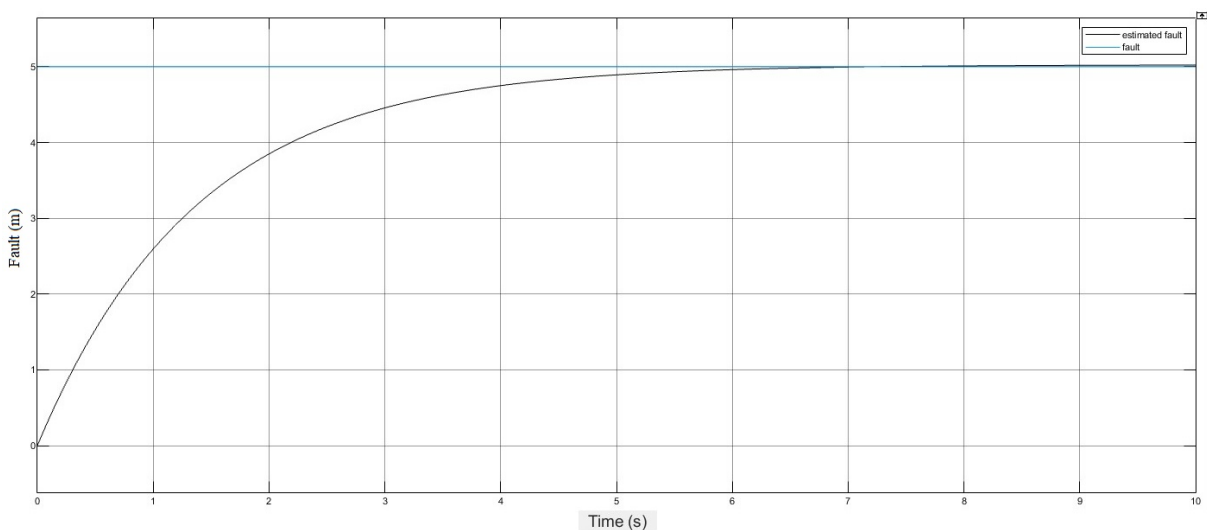

Figure 4.23: Sensor fault estimation with a PI observer
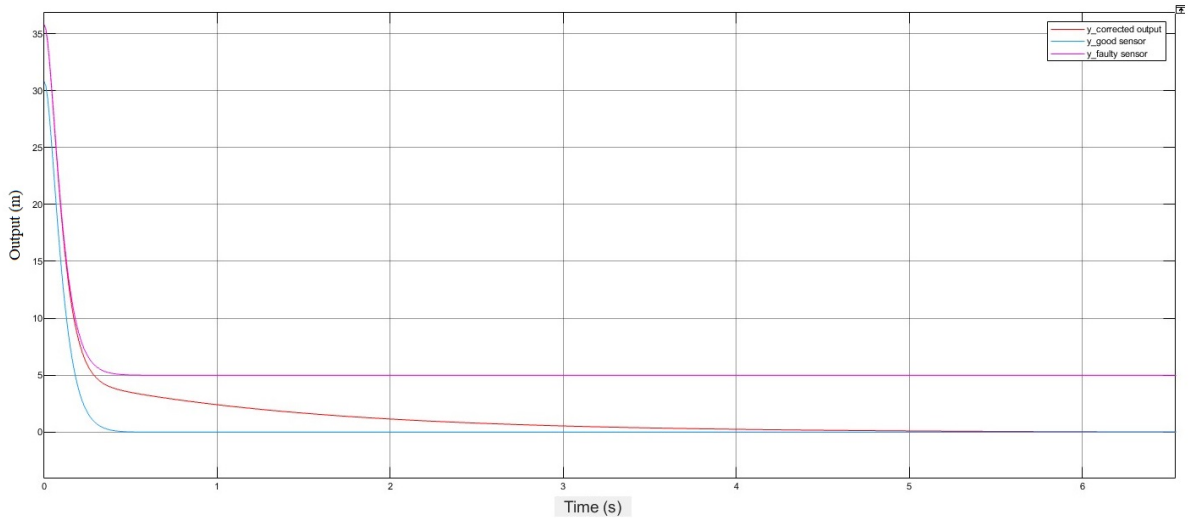

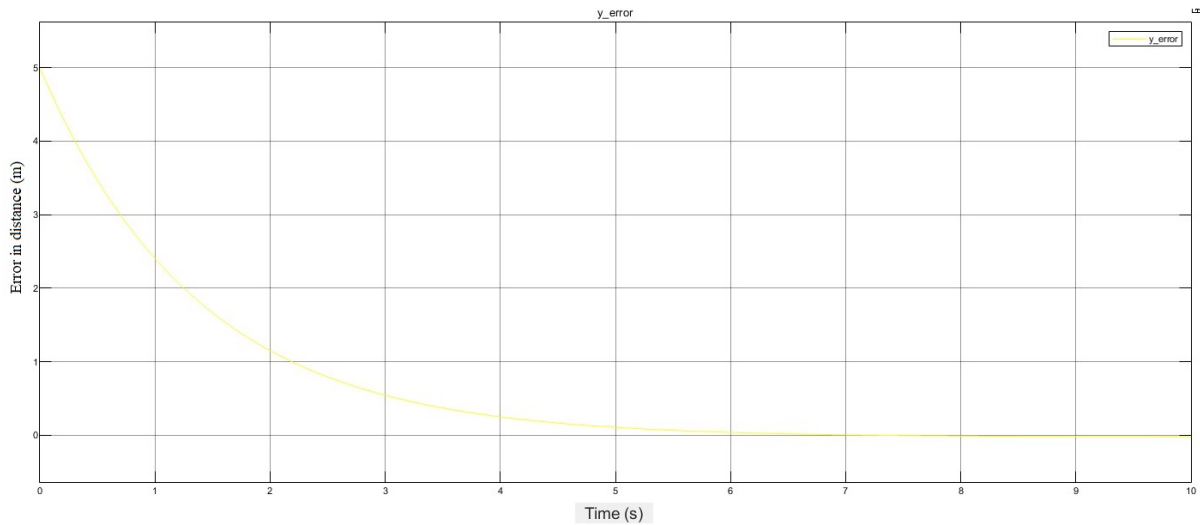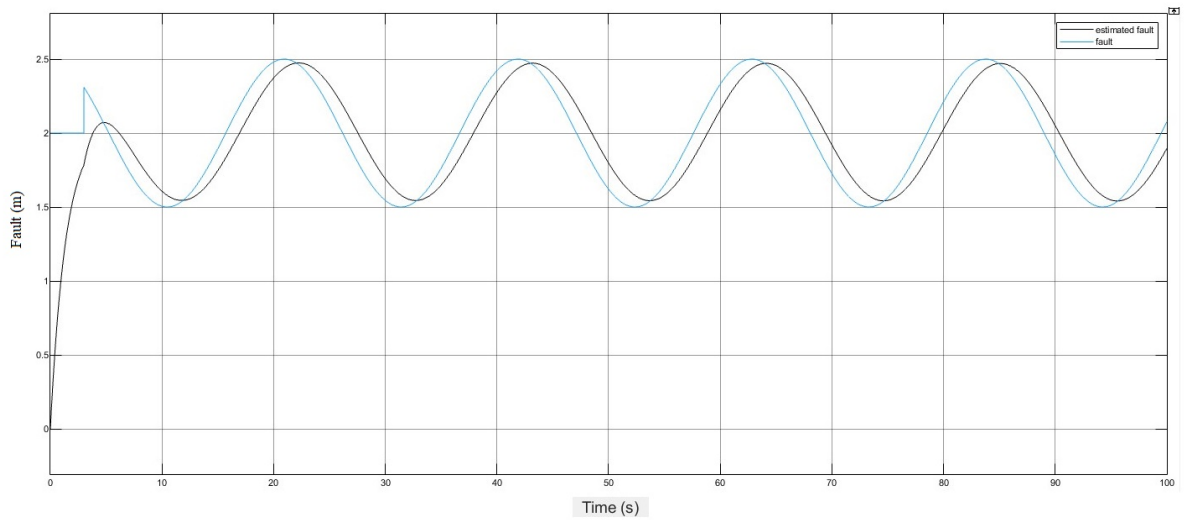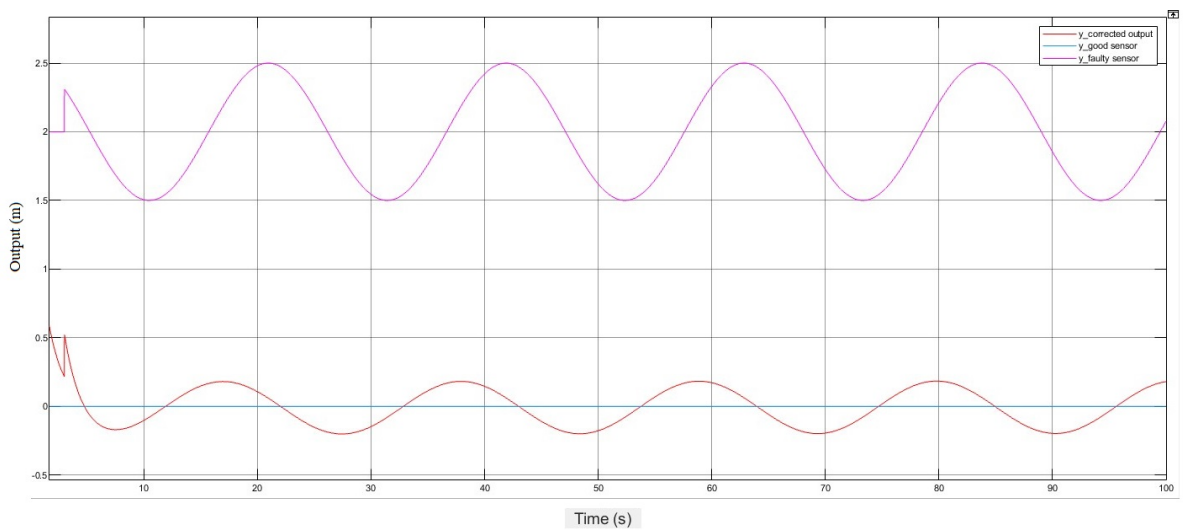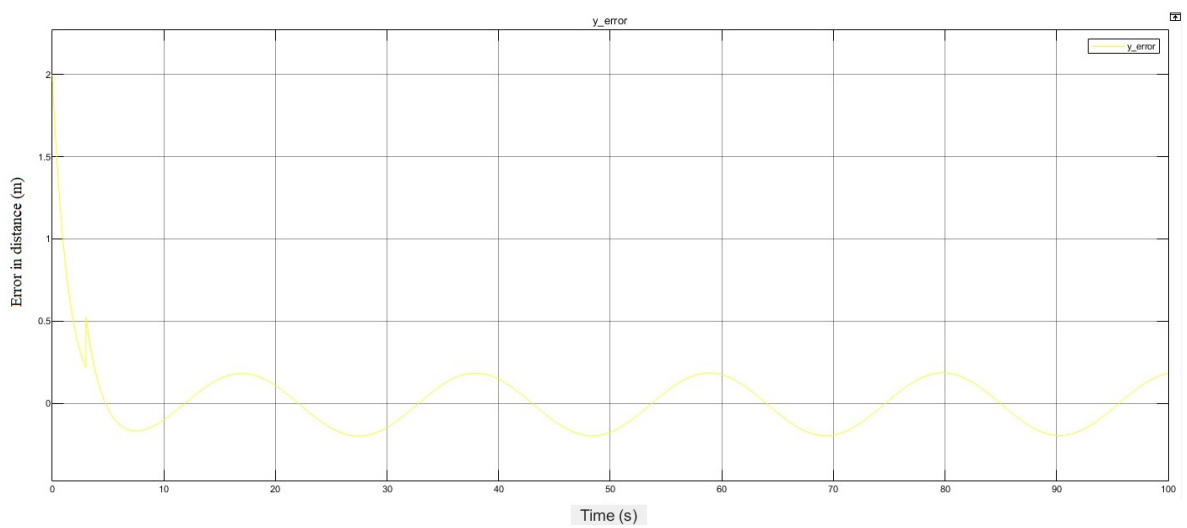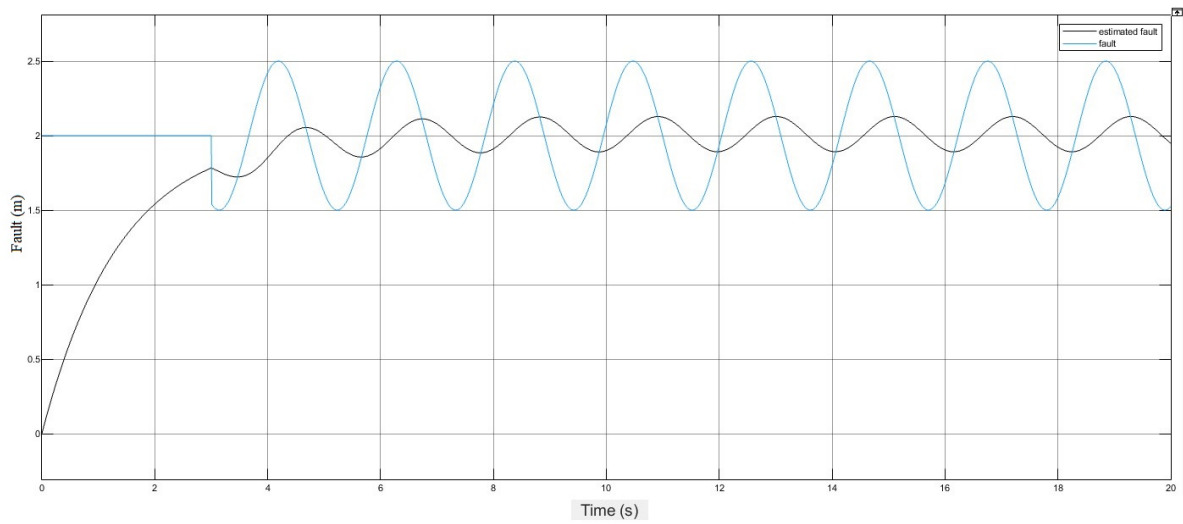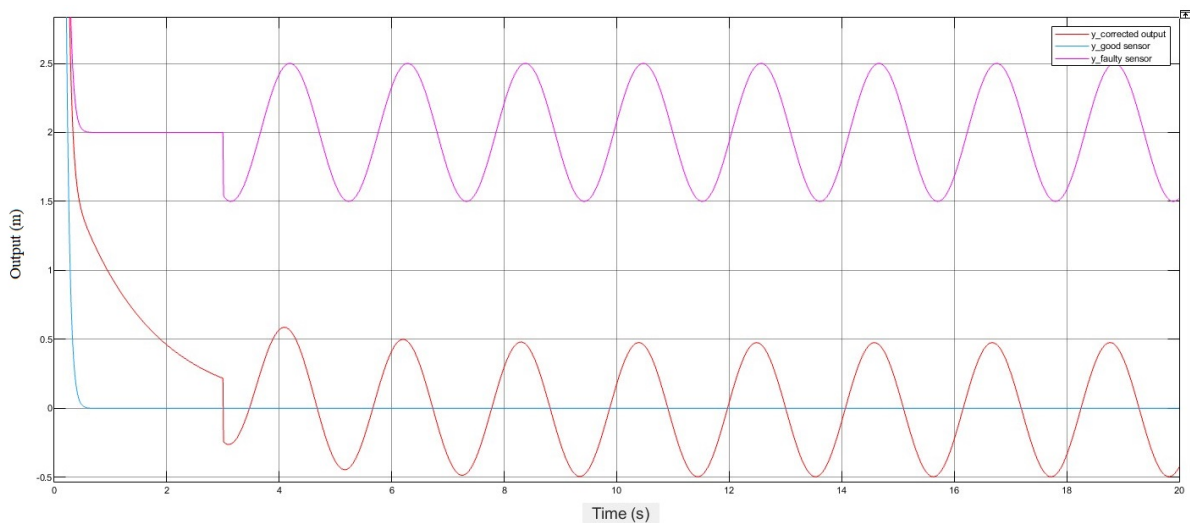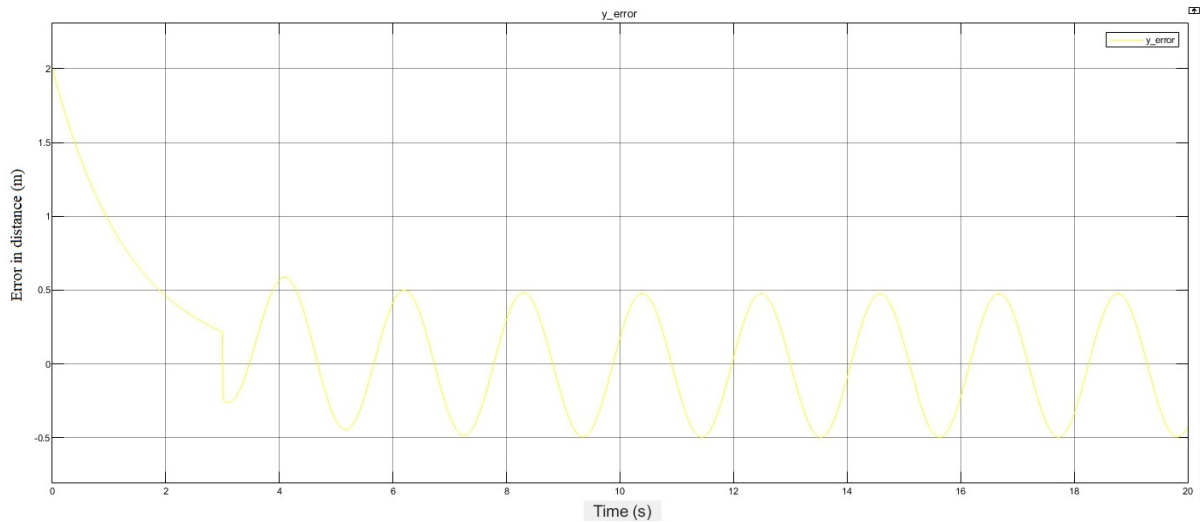Figure 4.24: Correction of the output in the presence of faults

Figure 4.25: Error between the output of good sensor and corrected output

Commentaries and conclusion

We observe that by injecting a constant fault $(\dot{d}(t) = 0)$, the PI observer is able to estimate it perfectly (error converges towards 0) with time of response of 6s (figure 4.17), the output is then corrected by FTC block and it converges towards the output given by a good sensor (figures 4.18 and 4.19).
Then, by adding a varying fault $(\dot{d}(t) \neq 0)$ to the constant fault, we observe that the PI observer is only able to estimate the constant fault perfectly (figures 4.20 and 4.23), and the performance of the estimation is based on the frequency of the signal. As consequence, only the effect of varying fault appears in the corrected output (figures 4.21 and 4.24). We notice that in case of slowly varying faults, the amplitude has been decreased in the corrected output (figure 4.21), however in the case of quickly varying faults, the amplitude has remained unchanged.

As previously mentioned, the PI observer is theoretically dedicated to the reconstruction of constant signals, however, it can in some practical cases estimate slowly varying signals, when the frequency of the latter increases, the estimation quality begins to degrade, it is then necessary to resort to other methods that are able to estimate high frequency signals such as the PMI observer approach. .

We can see the effectiveness of the fault tolerant control, based on the PI observer and applied for fuzzy multi-models of type T-S, indeed, figure (4.17) shows the case of faults of bias type, theoretically, the PI observer is designed for the estimation of constant signals, figures (4.20) and (4.23) illustrate the case of varying faults, more or less quickly, the estimation can be acceptable when it is a slowly varying signal, the results begin to degrade with the increase of the frequency, the approach used proves to be a little limited in high frequencies, the idea of increasing the gains can be used to maintain or improve performance, but it risks causing instability, it is recommended in this case to use more efficient methods and more robust observers including the PMI observer developed for a larger set of signals. However, the controller used could keep a certain robustness, in addition, it is a stabilization, the set point is always constant (stabilization at the origin),

the states are just deviated or deviated from their desired positions when a fault occurred, the application the application of the FTC command allows to remedy these faults. the application can be extended for the case of trajectory tracking.

4.6 Fault tolerant control by trajectory tracking

The main idea of assuring trajectory tracking with fault tolerant control is to use the command signal u(t) used in section (4.4) that allows the trajectory tracking only, and to also use both the PI observer and the FTC bloc used in section (4.5). Then, we combine both techniques using equation (3.19) (see figure 3.5) to achieve the desired objectives.

4.7 Conclusion

This last chapter was devoted to the application of the previously developed controls to a T-S type fuzzy model of an EV. The modeling of the EV has resulted in a nonlinear model. This model is then used to obtain the fuzzy multi-model representation of TS type. The PDC control law presented in the second chapter has been applied to stabilize the EV, then the application has been extended to realize a tracking of a given trajectory. In the last part, the techniques of fault diagnosis and fault tolerant control were used to develop stabilizing control laws in the presence of sensor faults. The combination of fuzzy control techniques and fault diagnosis techniques allowed the synthesis of fault tolerant controls allowing the stabilization of the system.

General conclusion

The objective of this work is to apply fault tolerant control techniques to nonlinear systems described by fuzzy multi-models of Takagi-Sugeno type, it is a consequence of the combination of several approaches and methods, indeed, we have involved modeling, control and fault diagnosis techniques to achieve this objective. The application has treated the case of a non-linear model to regulate the safety distance of an electric vehicle in circulation.

Within the framework of the modeling of the nonlinear systems by the fuzzy multi-model approach of T-S type, we considered only the case of the measurable premise variables, however the study can be widened towards the case of the non-measurable premise variables, a term will be generated by the difference between the activation functions according to the measured variables in the measurable case and those according to the estimated values in the contrary case, this term will be regarded as a disturbance to be imperatively taken into account at the time of the necessary developments. In this same context of modeling by T-S approach, we are interested in the study and the analysis of the stability of the fuzzy multi-models thus obtained, constraints and sufficient conditions of stability were given in chapter 2 in the form of LMIs, in addition, we also considered the case of unstable systems, and we used the PDC method for their stabilization by state feedback, we extended the work to try to realize a trajectory tracking, the designed fuzzy controller is based on the same fuzzy set as the system represented by the T-S multi-model approach, this approach also allows to apply and approach also allows to apply and extend methods of linear automatics to the nonlinear case, which is powerful and brilliant from a practical point of view. A placement of poles in LMI regions to ensure the desired stability and closed-loop performance has been presented in detail at the end of Chapter 2..

In the context of fault diagnosis, especially estimation, the approach adopted is based on the simultaneous estimation of the system state and the faults, through a PI observer, built by solving the LMI constraints presented in chapter 3, this estimation is the result of the diagnosis made by the FDI block, It will be used later by a second FTC block to compensate the faults and to compensate the faults and to elaborate the fault-tolerant control law.

The last chapter was dedicated to the application of the concepts presented and the results obtained in the previous chapters to a nonlinear system which is the EV. We found the effectiveness of the approaches used, the results obtained were generally acceptable, however they can be improved. Indeed, the stability constraints of the multimodels were conservative, we can use ralaxation theorems to allow the algorithm to search in larger domains in the hope of finding better solutions, so, in the case of tracking, sometimes

the designed controller has limitations especially when the references are at high frequency, the same remark was observed for the PI observers when the unknown inputs to be estimated vary faster since theoretically they are designed for constant signals, the manipulation of the LMIs and the constraints can be used to confront this but sometimes leads to the increase of the gains, which improves the speed and the performances but risks to provoke oscillations, overshootings or even instability, we then propose to use more powerful approaches, for example the PMI observers which allow to cover a wider class of signals which can be estimated simultaneously, another interesting strategy which we noticed, which is the use of a bank of observers to improve the quality and the precision of the estimation and also allows to avoid the false alarms.

Bibliography

[1]   J. Larminie and J. Lowry, *Electric vehicle technology explained.* John Wiley & Sons, 2012.

[2]   Z. Gelmanova, G. Zhabalova, G. Sivyakova, *et al.*, "Electric cars. advantages and disadvantages," in *Journal of Physics: Conference Series*, IOP Publishing, vol. 1015, 2018, p. 052 029.

[3]   M. H. Westbrook and M. Westbrook, *The Electric Car: Development and future of battery, hybrid and fuel-cell cars*, 38. Iet, 2001.

[4]   P.-F. Toulotte, "Attelage virtuel pour véhicules automatisés," Ph.D. dissertation, Université de Valenciennes et du Hainaut-Cambresis, 2006.

[5]   B. de Mostaganem, M. Y. Abdellah, and M. C. Abdellah, "Étude comparative entre influence des déférent parámétrer physique et la performance du véhicule électrique modélisation et simulation,"

[6]   K. Tanaka and H. O. Wang, *Fuzzy control systems design and analysis.* Wiley Online Library, 2001.

[7]   M. Chadli, "Stabilité et commande de systèmes décrits par des multimodèles," Ph.D. dissertation, Institut National Polytechnique de Lorraine, 2002.

[8]   D. Ichalal, "Estimation et diagnostic de systèmes non linéaires décrits par un modèle de takagi-sugeno," Ph.D. dissertation, Institut National Polytechnique de Lorraine, 2009.

[9]   M. Chilali and P. Gahinet, "H/sub/spl infin//design with pole placement constraints: An lmi approach," *IEEE Transactions on automatic control*, vol. 41, no. 3, pp. 358–367, 1996.

[10]   P.-F. Toulotte, S. Delprat, T.-M. Guerra, and J. Boonaert, "Vehicle spacing control using robust fuzzy control with pole placement in lmi region," *Engineering Applications of Artificial Intelligence*, vol. 21, no. 5, pp. 756–768, 2008.

[11]   R. J. Patton, J. Chen, and C. Lopez-Toribio, "Fuzzy observers for nonlinear dynamic systems fault diagnosis," in *Proceedings of the 37th IEEE Conference on Decision and Control (Cat. No. 98CH36171)*, IEEE, vol. 1, 1998, pp. 84–89.

[12]   O. Kraa, M. Becherif, M. Ayad, *et al.*, "States feedback control applied to the electric vehicle," *Energy Procedia*, vol. 50, pp. 186–193, 2014.

[13]   E. Helmers and P. Marx, "Electric cars: Technical characteristics and environmental impacts," *Environmental Sciences Europe*, vol. 24, no. 1, pp. 1–15, 2012.

Bibliography

[14] C. Espanet, "Modélisation et conception optimale de moteurs sans balais à structure inversée-application au moteur-roue," Ph.D. dissertation, Université de Franche-Comté, 1999.

[15] G. Paganelli, "Conception et commande d'une chaîne de traction pour véhicule hybride parallèle thermique et électrique," Ph.D. dissertation, Valenciennes, 1999.

[16] L. Nouveliere, E. DUPONT-KERLAN, and H. Fontaine, "Commandes robustes appliquées au contrôle assisté d'un véhicule à basse vitesse," in *COLLOQUE FEMMES ET VILLES, 8 ET 9 MARS 2002, TOURS*, 2002.

[17] I. Ellouze, "Etude de la stabilité et de la stabilisation des systèmes à retard et des systèmes impulsifs," Ph.D. dissertation, Université Paul Verlaine-Metz; Université de Sfax, 2010.

[18] J. Zhang, A. K. Swain, and S. K. Nguang, *Robust observer-based fault diagnosis for nonlinear systems using MATLAB®*. Springer, 2016.

[19] M. Doublet, "Commande tolérante aux défauts et diagnostic des systèmes à retard inconnu par une approche sans modèle," Ph.D. dissertation, Université de Lorraine, 2018.

[20] D. Kharrat, "Commande tolérante aux défauts des systèmes non linéaires: Application à la dynamique du véhicule," Ph.D. dissertation, Université de Picardie Jules Verne; Université de Sfax (Tunisie), 2019.

[21] S. Aouaouda, M. Chadli, V. Cocquempot, and M. Tarek Khadir, "Multi-objective h-/ h∞ fault detection observer design for takagi–sugeno fuzzy systems with unmeasurable premise variables: Descriptor approach," *International Journal of Adaptive Control and Signal Processing*, vol. 27, no. 12, pp. 1031–1047, 2013.

[22] M. Blanke, M. Kinnaert, J. Lunze, M. Staroswiecki, and J. Schröder, *Diagnosis and fault-tolerant control*. Springer, 2006, vol. 2.

[23] I. H. Brahim, M. Bouattour, M. Chaabane, and D. Mehdi, "Fault tolerant controller design for ts fuzzy system using descriptor approach with application to a three tank system,"

[24] B. Boussaïd, "Contribution à la tolérance active aux défauts des systèmes dynamiques par gestion des références," Ph.D. dissertation, Université Henri Poincaré-Nancy 1, 2011.

[25] F. Chen, L. Hu, and C. Wen, "Improved adaptive fault-tolerant control design for hypersonic vehicle based on interval type-2 t-s model," *International Journal of Robust and Nonlinear Control*, vol. 28, no. 3, pp. 1097–1115, 2018.

[26] L. Chen, X. Huang, and M. Liu, "Fault-tolerant control against simultaneous partial actuator degradation and additive sensor fault," in *2017 American Control Conference (ACC)*, IEEE, 2017, pp. 4105–4110.

[27] H. Dahmani, O. Pagès, A. El Hajjaji, and N. Daraoui, "Observer-based robust control of vehicle dynamics for rollover mitigation in critical situations," *IEEE Transactions on Intelligent Transportation Systems*, vol. 15, no. 1, pp. 274–284, 2013.

[28] P. Cheng, Z. Gao, Z. Zhou, M. Qian, and J. Lin, "Active ftc approach design for a class of nonlinear flight control systems with actuator faults," in *2017 29th Chinese Control And Decision Conference (CCDC)*, IEEE, 2017, pp. 6474–6479.

[29]   C. Edwards and C. P. Tan, "Sensor fault tolerant control using sliding mode observers," *Control Engineering Practice*, vol. 14, no. 8, pp. 897–908, 2006.

[30]   A. El Hajjaji, M. Chadli, M. Oudghiri, and O. Pages, "Observer-based robust fuzzy control for vehicle lateral dynamics," in *2006 American Control Conference*, IEEE, 2006, 6–pp.

[31]   R. Fonod, D. Henry, C. Charbonnel, and E. Bomschlegl, "A class of nonlinear unknown input observer for fault diagnosis: Application to fault tolerant control of an autonomous spacecraft," in *2014 UKACC International Conference on Control (CONTROL)*, IEEE, 2014, pp. 13–18.

Appendixes

Solving Linear Matrix Inequality (LMI) Problems

In this section, we present a brief introduction about linear matrix inequalities which have been used extensively to solve problems described in this work.

Introduction to LMI

LMIs are matrix inequalities which are linear or affine in a set of matrix variables. They are essentially convex constraints and therefore many optimization problems with convex objective functions and LMI constraints can easily be solved efficiently using many existing software. This method has been very popular among control engineers in recent years. This is because a wide variety of control problems can be formulated as LMI problems. An LMI has the following form:

$$F(x) = F_0 + x_1 F_1 + ... + x_n F_n = F_0 + \sum_{i=1}^{n} x_i F_i > 0$$

where $x \in R^m$ is the vector of decision variables and $F_0, F_1, ..., F_n$ are given constant symmetric real matrices, i.e., $F_i = F_i^T$, i = 0,..., m. The inequality symbol in the equation means F(x) is positive definite, i.e., $u^T F(x) u > 0$ for all nonzero $u \in R^n$. This matrix inequality is linear in the variables x_i.

As an example, the Lyapunov inequality: $A^T P + PA < 0$

where $A \in R^{n \times n}$ is given and P is a symmetrix matrix $n \times n$

Tricks used in LMIs

Although many problems in control can be formulated as LMI problems, some of these problems result in nonlinear matrix inequalities. There are certain tricks which can be used to transform these nonlinear inequalities into suitable LMI forms. Some of the tricks which are often used in control are described here with suitable examples.

Change of variables

By defining new variables, it is sometimes possible to linearize nonlinear matrix inequalities.

Example of synthesis of state feedback controller: The objective is to determine a matrix

$F \in R^{m \times n}$ such that all the eigenvalues of the matrix $A + BF$ $R^{n \times n}$ lie in the open left-half of the complex plane. Using Lyapunov theory, it can be shown that this is equivalent to find a matrix F and a positive definite matrix $P \in R^{n \times n}$ such that the following inequality holds:

$$(A + BF)^T P + P(A + BF) < 0 A^T P + PA + F^T B^T P + PBF < 0$$

Note that the terms with products of F and P are nonlinear or bilinear.
By defining new variables : $Q = P^{-1}$ and $L = FQ$ we obtain:

$$QA^T + AQ + L^T B^T + BL < 0$$

This gives an LMI feasibility problem in the new variables $Q > 0$ and $L \in R^{m \times n}$. After solving this LMI, the feedback matrix F and Lyapunov variable P can be recovered from $F = LQ^{-1}$ and $P = Q^{-1}$. This shows that by making a change of variables, we can obtain an LMI from a nonlinear matrix inequality.

The Schur Complement

Schur's formula is used in transforming nonlinear inequalities of convex type into LMI. This says that the LMI:

$$\begin{bmatrix} Q(x) & S(x) \\ S(x)^T & R(x) \end{bmatrix} < 0$$

where $Q(x) = Q(x)^T$, $R(x) = R(x)^T$ and S(x) depends affinely on x, is equivalent to:

$$R(x) < 0 , \ Q(x) - S(x)R(x)^{-1}S(x)^T < 0.$$

Example: Consider the following matrix inequality:

$$A^T P + PA + PBR^{-1}B^T P + Q < 0,.$$

where $P = P^T > 0$ and $R > 0$, is equivalent to:

$$\begin{bmatrix} A^T P + PA + Q & PB \\ B^T P & -R \end{bmatrix} < 0$$

Solving LMI Using MATLAB Toolbox

The LMI toolbox of MATLAB provides a set of useful functions to solve LMIs. Some of these functions are discussed here with sample codes. **Step-1: Initialization** At the

beginning, initialize the LMI description with the command setlmis([]). Note that this function does not take any parameter.

Step-2: Defining the Decision Variables Next, it is necessary to define the decision variables, i.e., the unknown variables of the LMI problem. As an example, consider the LMI $C^T X C < 0$, where C is a constant matrix and X is the matrix of decision variables. It is defined using the function lmivar which has the following syntax:

$$X = \text{lmivar(type, structure)}$$

This command allows us to define several forms of decision matrices such as symmetrical matrices, rectangular matrices or matrices of other type. Depending on the selected matrix type, the structure contains different information. Thus, first we define the type and then define the structure which depends on the type.

-If type = 1, this implies that the matrix X is square and symmetrical. The structure element (i, 1) specifies the dimension of the ith-block, while structure element (i, 2) specifies the type of the ith-block (1 for full, 0 for scalar and -1 for zero block).

-If type = 2, matrix X is rectangular of size m × n as specified in structure = [m, n].

-If type = 3, matrix X is of other type

Step-3: Define the LMIs one by one This is done with the command lmiterm. The syntax of the command is:

$$\text{lmiterm(termID, A, B, flag)}$$

The lmiterm takes 3 or 4 arguments. The first argument term ID is a 1 × 4 vector. The first element of this vector indicates which LMI is defined. The second and third entry in this vector gives the position of the term being defined. And the fourth entry indicates which LMI decision variable is involved. It can be 0, X or X^T depending on whether the term is constant, of type AXB or AX^TB. The second and third arguments of lmiterm function are the left and right multiplier of the decision matrix. If the flag is set to 's', it permits to specify with a single command that the given term and its symmetrical appears in the LMI.

Example: Consider the following set of LMIs:

$$\begin{bmatrix} CX^TC^T + B^TYA & XF \\ F^TXY & \end{bmatrix}$$

$$DXD^T > 0$$

Here we have two decision variables X and Y, and two LMIs. Let Y be a full symmetric matrix of dimension 5 and X has 5 blocks and the dimensions of the various block matrices are 5, 4, 3, 1 and 2.

First, we define the variables X and Y using lmivar function as follows:

```
structureX=[5,1;4,1;3,1;1,0;2,1];
X=lmivar(1,structureX);

structureY=[5,1];
Y=lmivar(1,structureY);
```

Then, we define the LMIs using lmiterm function as follows:

```
% LMI (A.15)
lmiterm([1 1 1 X],C,C');            % This represents term CXC'
lmiterm([1 1 1 Y],B',A);            % This represents the term B'
    YA
lmiterm([1 1 2 X],1,F);                % This represents term XF
lmiterm([1 2 1 X],F',1);               % This represents term F'
    X
lmiterm([1 2 2 Y],1,1);                % This represents term Y

% LMI (A.16)
lmiterm([-1,1,1,X],D,D');              % Term DXD > 0
```

Lastly, we create an LMI object using the following command.

```
myLMIsystem=getlmis;
```

Simulink schematic diagrams

Figure 26: Simulation of inter-vehicle distance control

Figure 27: Simulation of fault tolerant control